Article

Large Deflection Analysis of Peripherally Fixed Circular Membranes Subjected to Liquid Weight Loading: A Refined Design Theory of Membrane Deflection-Based Rain Gauges

Jun-Yi Sun [1,2,*] **, Qi Zhang** [1] **, Ji Wu** [1] **, Xue Li** [1] **and Xiao-Ting He** [1,2]

[1] School of Civil Engineering, Chongqing University, Chongqing 400045, China; 202016021045@cqu.edu.cn (Q.Z.); 202116131099t@cqu.edu.cn (J.W.); 20161602025t@cqu.edu.cn (X.L.); hexiaoting@cqu.edu.cn (X.-T.H.)
[2] Key Laboratory of New Technology for Construction of Cities in Mountain Area (Chongqing University), Ministry of Education, Chongqing 400045, China
* Correspondence: sunjunyi@cqu.edu.cn; Tel.: +86-(0)23-65120720

Abstract: The anticipated use of elastic membranes for deflection-based rain gauges has provided an impetus for this paper to revisit the large deflection problem of a peripherally fixed circular membrane subjected to liquid weight loading, a statics problem when the fluid–structure interaction of membrane and liquid reaches static equilibrium. The closed-form solution of this statics problem of fluid–structure interaction is necessary for the design of such membrane deflection-based rain gauges, while the existing closed-form solution, due to the use of the small rotation angle assumption of the membrane, cannot meet the design requirements for computational accuracy. In this paper, the problem under consideration is reformulated by giving up the small rotation angle assumption, which gives rise to a new and somewhat intractable nonlinear integro-differential equation of the governing out-of-plane equilibrium. The power series method has played an irreplaceable role in analytically solving membrane equations involving both integral and differential operations, and a new and more refined closed-form solution without the small rotation angle assumption is finally presented. Numerical examples conducted show that the new and more refined closed-form solution presented has satisfactory convergence, and the effect of giving up the small rotation angle assumption is also investigated numerically. The application of the closed-form solution presented in designing such membrane deflection-based rain gauges is illustrated, and the reliability of the new and more refined closed-form solution presented was confirmed by conducting a confirmatory experiment.

Keywords: circular membrane; liquid weight loading; fluid–structure interaction; integro-differential equation; power series method; closed-form solution

1. Introduction

Membranes are increasingly being used in a wide variety of applications [1–4]. In our earlier work [5], the statics problem of fluid–structure interaction of a peripherally fixed circular membrane subjected to liquid weight loading is investigated analytically. The mathematical formulation of this problem results in a boundary value problem including both differential operation and integral operation, and the resulting integro-differential equations are successfully solved by using the power series method. Our primary motivation for investigating this fluid–structure interaction problem is to provide the closed-form solution needed for the development of a new type of membrane deflection-based rain gauge, a device for collecting and measuring the amount of rain which falls. In this study, the statics problem of fluid–structure interaction addressed in [5] is reformulated and solved, with an aim of giving a more refined closed-form solution than that given in [5], which is essential for the development of this membrane deflection-based rain gauge.

Many membranes can exhibit large elastic deflection under transverse loading [6–8], which provides the possibility for the development of deflection measurement-based devices [9–13]. Figure 1 shows the circular rainwater storage container of the membrane deflection-based rain gauge to be developed, a vertically placed rigid round tube of finite length with an inner radius a, whose upper end is open and whose lower end is sealed by an initially flat, elastic circular membrane of radius $a\hat{}$ which is used as an elastic bottom. The circular membrane as the elastic bottom will exhibit elastic deflection as the rainwater collected is injected into the storage container from the upper open end. Obviously, the higher the height H of the rainwater stored in the container, the greater the maximum deflection w_m of the circular membrane, see Figure 1. If the circular membrane problem shown in Figure 1, i.e., the problem of axisymmetric deformation and deflection of the peripherally fixed circular membrane under liquid weight loading, can be analytically solved, then the analytical relationship between the maximum deflection w_m and the volume (or the height H) of the rainwater in the storage container can be obtained. Therefore, with the obtained analytical relationship, the volume (or the height H) of the rainwater in the storage container can be determined by measuring the maximum deflection w_m. The frequency (or time interval) of measuring the maximum deflection w_m can be as small or as large as desired, that is, the maximum deflection w_m can be measured once per second or minute or hour, providing convenience for different measurement data requirements. The rainfall per unit of time can be determined by two sets of measurement data, i.e., by the change in the volume (or the height H) of the rainwater in the storage containers divided by the time intervals of the two sets of measurement data. The rainfall per unit of time is calculated usually in minutes for rainstorms or heavy rain and usually in hours for moderate or light rain, but sometimes the volume of rainfall of moderate or light rain per minute also needs to be known. Therefore, it is best for rainfall to be measured in a continuous manner. However, traditional tipping bucket rain gauges (TBRGs) cannot achieve continuous measurement of rainfall, because the time it takes to fill a TBRG bucket with rainwater depends entirely on rainfall intensity [14,15]. Obviously, a TBRG bucket that can be filled with rainwater in a minute during light rain is not suitable for measuring the rainfall of rainstorm or heavy rain, because the volume of the bucket is too small and the tipping occurs too quickly during heavy rain, especially in a rainstorms. The advantage of the membrane deflection-based rain gauge proposed in this paper is that continuous measurements can be easily achieved (so, the rainfall per minute or hour can be easily given, regardless of whether one is measuring a rainstorm, heavy rain, moderate rain or light rain), but only if a closed-form solution can be given for the circular membrane problem in Figure 1.
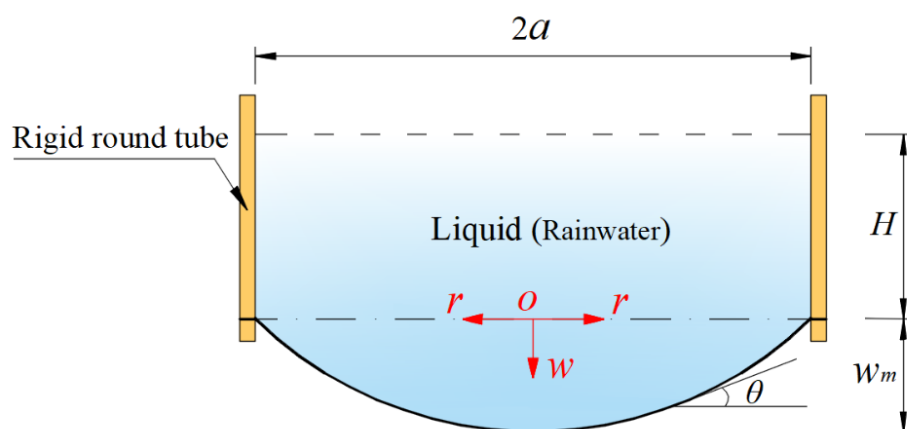

Figure 1. Geometry of the circular membrane under liquid weight loading.

Therefore, the key problem to be solved is to give the closed-form solution for the circular membrane problem shown in Figure 1. The large deflection phenomenon of

membranes usually gives rise to nonlinear equations when formulated mathematically, and these nonlinear equations are generally difficult to address analytically [16–21]. In the existing literature, almost all analytical solutions for circular membrane problems are applicable only to the case of uniform loading, that is, loads applied onto the surface of circular membranes are always uniformly distributed regardless of membrane deflection [22–29]. However, shown in Figure 1, the loads (the liquid, rainwater) applied onto the surface of the circular membrane are not uniformly distributed. The nonuniformity of the liquid distributed on the circular membrane will vary with the height H of the liquid stored in the container. In other words, liquid applied onto the surface of the initially flat circular membrane gives rise to the deflection of the circular membrane, while in turn the shape of the deflected circular membrane determines the distribution of the liquid over the deflected circular membrane, i.e., the distribution of the loads acting on the deflected circular membrane. Therefore, there is an interaction between the action field of the fluid (rainwater) and the response field of the solid (membrane), resulting in the fluid–structure interaction or coupling phenomenon. Obviously, for a given quantity of liquid (i.e., the total volume of the rainwater injected into the storage container remains unchanged), the two-phase coupling interface will eventually reach static equilibrium, resulting in a statics problem of fluid–structure interaction.

This statics problem of fluid–structure interaction is analytically addressed in [5] for the first time, where the out-of-plane equilibrium equation, in-plane equilibrium equation, geometric equations and physical equations are established, and a closed-form solution of the problem is presented. The out-of-plane equilibrium equation is obtained by the equilibrium condition in the direction perpendicular to the initially flat circular membrane, while the in-plane equilibrium equation is obtained by the equilibrium condition in the direction parallel to the initially flat circular membrane. The geometric equations refer to the relationship between the strain and displacement of the deflected circular membrane, while the physical equations refer to the physical relationship between stress and strain following the generalized Hooke's law. In [5], the out-of-plane equilibrium equation established is an integro-differential equation involving both integral and differential operations, which makes it difficult to analytically solve the simultaneous equations of out-of-plane and in-plane equilibrium equations, geometric equations and physical equations. The power series method has played an irreplaceable role in overcoming the difficulty of analytically solving these simultaneous equations, and due to its successful use, the closed-form solution for these simultaneous equations is finally given. The research results in [5] show that the fluid–structure coupling effect is substantial when the height H of the liquid (rainwater) in the storage container is relatively small, but it slowly becomes weak as the height H increases.

However, it can be seen from [5] that the integro-differential equation governing the out-of-plane equilibrium (i.e., Equation (4) in [5]) is actually derived under the small rotation angle assumption of a membrane—the rotation angle of the deflected circular membrane, θ (see Figure 1), is assumed to be so small that $\sin\theta$ can be approximated by $\tan\theta$. That is, there exists an approximation of $\sin\theta = \tan\theta$ under the small rotation angle assumption of the membrane. For the problem under consideration, since $\tan\theta$ is equal to $-\mathrm{d}w/\mathrm{d}r$ (r is the radial coordinate and w is the deflection, as in Figure 1, $\sin\theta$ can be written as $\sin\theta = \tan\theta = -\mathrm{d}w/\mathrm{d}r$, i.e., Equation (3) in [5]. As is known to all, the exact relationship between $\sin\theta$ and $\tan\theta$ should be $\sin\theta = 1/(1 + 1/\tan^2\theta)^{1/2}$. Obviously, if $\sin\theta = 1/(1 + 1/\tan^2\theta)^{1/2} = 1/[1 + 1/(-\mathrm{d}w/\mathrm{d}r)^2]^{1/2}$ (rather than $\sin\theta = \tan\theta = -\mathrm{d}w/\mathrm{d}r$) is used to establish the out-of-plane equilibrium equation, then the resulting the integro-differential equation governing the out-of-plane equilibrium will become more complicated mathematically, which can be seen in subsequent derivations (see Equations (3) and (4) in this paper). The more complex out-of-plane equilibrium equation naturally makes it more difficult to simultaneously solve the out-of-plane and in-plane equilibrium equation, geometric equations and physical equations, which is why $\sin\theta = \tan\theta$ is used instead of $\sin\theta = 1/(1 + 1/\tan^2\theta)^{1/2}$ in [5].

Obviously, the use of small rotation angle assumption of a membrane using $\sin\theta = \tan\theta$ instead of $\sin\theta = 1/(1 + 1/\tan^2\theta)^{1/2}$, will inevitably lead to the loss of computational accuracy of the closed-form solution of the statics problem of fluid–structure interaction shown in Figure 1, especially when the rotation angle of the deflected circular membrane, θ, is relatively large, i.e., when the height H of the liquid injected into the storage container is relatively large. Therefore, the closed-form solution presented by [5] is suitable only for a case when the height H of the liquid injected into the storage container is relatively small. In other words, if it is used when the height H of the liquid injected into the storage container is relatively large, a large calculation error will be caused. For a membrane deflection-based rain gauge to be developed, however, the height H needs to be able to range from a very small value to a very large value, which means that a closed-form solution whose computational accuracy is not affected by the change in the height H, is necessary. The closed-form solution presented by [5] cannot meet the requirement to develop such membrane deflection-based rain gauges, due to the use of small rotation angle assumption of the membrane, that is, using $\sin\theta = \tan\theta$ instead of $\sin\theta = 1/(1 + 1/\tan^2\theta)^{1/2}$. Therefore, it is necessary to give up the small rotation angle assumption of the membrane, that is, using $\sin\theta = 1/(1 + 1/\tan^2\theta)^{1/2}$ (rather than $\sin\theta = \tan\theta$) during the derivation of the integro-differential equation governing the out-of-plane equilibrium. It can be seen from the following study that the closed-form solution which is obtained by giving up the small rotation angle assumption of the membrane does have the desired effect. The main aim of this study is to provide a closed-form solution without small rotation angle assumption, whose computational accuracy is not affected by change in the height H, in order to meet the requirement of developing such membrane deflection-based rain gauges.

In the following section, the fluid–structure interaction problem in Figure 1 is reformulated under the condition of using $\sin\theta = 1/(1 + 1/\tan^2\theta)^{1/2}$, resulting in a new and more complicated integro-differential equation governing the out-of-plane equilibrium. The problem reformulated is solved by using the power series method and a new, more refined closed-form solution of the problem is finally presented. In Section 3, some important issues are discussed, such as the validity and convergence of the closed-form solution presented. The variation of the difference between the closed-form solutions presented by [5] and by this paper with the increase of the height H is analyzed numerically. The application of the closed-form solution presented in designing such membrane deflection-based rain gauges is illustrated. In addition, in order to verify the validity of the closed-form solution presented, a confirmatory experiment is conducted. Concluding remarks are given in Section 4.

2. Membrane Equation and Its Solution

The circular rainwater storage container of the membrane deflection-based rain gauge to be developed is as shown in Figure 1, where a rigid round tube of finite length with inner radius a is placed vertically, such that the upper end of the round tube is open and the lower end of the round tube is sealed by an initially flat, elastic circular membrane with Young's modulus of elasticity E, Poisson's ratio v and thickness h to form a soft bottom with the ability of elastic deformation, the rainwater collected is injected into the storage container from the upper end, and the maximum elastic deflection of the circular membrane eventually reaches w_m when the height of the rainwater stored in the container reaches H.

A piece of the central portion circular membrane whose radius is $0 \le r \le a$ is taken as a free body to study its static problem of equilibrium, as shown in Figure 2, where the origin o of the introduced cylindrical coordinate system (r, φ, w) is placed in the centroid of the geometric intermediate plane of the initially flat circular membrane, the polar coordinate plane (r, φ) is placed in the plane in which the geometric middle plane is located, r denotes the radial coordinate, φ denotes the circumferential angle coordinate which is not represented in Figure 2 due to the axisymmetry of the problem under consideration, w denotes the axial coordinate as well as the transverse displacement of the deflected circular

membrane, θ denotes the rotation angle of the deflected circular membrane, σ_r denotes the radial stress, and $q(r)$ denotes the transverse loads that varies continuously with the radial coordinate r (i.e., the liquid acting on the surface of the deflected circular membrane, which is distributed uniformly in the circumferential direction and unevenly in the radial direction and can thus be represented as a function of the r).
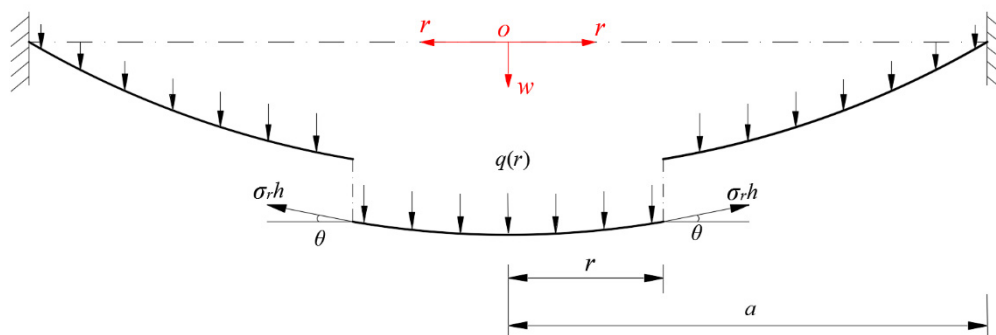

Figure 2. Sketch of a free body with radius $0 \leq r \leq a$. Adapted from Refs. [18,29].

The free body shown in Figure 2 is subjected to the joint actions of the external action force $F(r)$ produced by the transverse loads $q(r)$ within radius r and the total force $2\pi r\sigma_r h$ produced by the membrane force $\sigma_r h$ acting on the boundary r. Obviously, the external force $F(r)$ produced by $q(r)$ within r is equal to the weight of the liquid within r, and is given by

$$F(r) = \rho g \int_0^r [w(r) + H] \cdot 2\pi r \mathrm{d}r = 2\pi \rho g \int_0^r w(r) r \mathrm{d}r + \rho g \pi r^2 H, \tag{1}$$

where $w(r)$ is the transverse displacement of the deflected circular membrane at r, ρ is the liquid density and g is the acceleration of gravity. The direction of $F(r)$ is always vertically downward, that is, is always perpendicular to the initially flat circular membrane, while the vertical upward force is equal to $2\pi r\sigma_r h\sin\theta$, that is the vertical component of the force $2\pi r\sigma_r h$ at r. Therefore, after ignoring the weight of the circular membrane, the equilibrium condition where the resultant force in the vertical direction is equal to zero gives

$$2\pi r\sigma_r h \sin\theta = F(r) = 2\pi \rho g \int_0^r w(r) r \mathrm{d}r + \rho g \pi r^2 H, \tag{2}$$

where

$$\sin\theta = 1/\sqrt{1 + 1/\tan^2\theta} = 1/\sqrt{1 + 1/(-\mathrm{d}w/\mathrm{d}r)^2}. \tag{3}$$

Substituting Equation (3) into Equation (2) yields

$$\frac{2r\sigma_r h}{\sqrt{1 + 1/(-\mathrm{d}w/\mathrm{d}r)^2}} = 2\rho g \int_0^r w(r) r \mathrm{d}r + \rho g r^2 H. \tag{4}$$

In [5], this expression, which corresponds to Equation (3) in this paper, is given by $\sin\theta = \tan\theta = -\mathrm{d}w/\mathrm{d}r$, i.e., Equation (3) in [5]. It can be seen by comparing Equation (3) in this paper with Equation (3) in [5] that the approximation of replacing $\sin\theta = 1/(1 + 1/\tan^2\theta)^{1/2}$ with $\sin\theta = \tan\theta$ has been discarded in this paper. Equation (4) is the fluid–structure coupling equation at static equilibrium, which is usually known as the out-of-plane equilibrium equation. Obviously, this integro-differential equation governing the out-of-plane equilibrium is much more complicated than the one presented in [5] (i.e., Equation (4) in [5]).

The in-plane equilibrium equation can be established by the equilibrium condition of the resultant force in the horizontal direction being equal to zero, and may be written as

$$\frac{\mathrm{d}}{\mathrm{d}r}(r\sigma_r h) - \sigma_t h = 0, \tag{5}$$

where σ_t denotes the circumferential stress and $\sigma_t h$ is the circumferential membrane force.

Suppose that the radial strain is denoted by e_r, the circumferential strain is denoted by e_t and the radial displacement is denoted by u. Then, the geometric equations, the relations of strain and displacement, may be written as [22,23]

$$e_r = \frac{\mathrm{d}u}{\mathrm{d}r} + \frac{1}{2}\left(\frac{\mathrm{d}w}{\mathrm{d}r}\right)^2 \tag{6}$$

and

$$e_t = \frac{u}{r}. \tag{7}$$

In addition, the membrane is still assumed to be a linearly elastic or Hooke-type material. Thus the physical equations (i.e., the relations of stress and strain) follow the generalized Hooke's law

$$\sigma_r = \frac{E}{1 - v^2}(e_r + v e_t) \tag{8}$$

and

$$\sigma_t = \frac{E}{1 - v^2}(e_t + v e_r). \tag{9}$$

Eliminating e_r and e_t in Equations (8) and (9) by substituting Equations (6) and (7) into Equations (8) and (9) yields

$$\sigma_r = \frac{E}{1 - v^2}\left[\frac{\mathrm{d}u}{\mathrm{d}r} + \frac{1}{2}\left(\frac{\mathrm{d}w}{\mathrm{d}r}\right)^2 + v\frac{u}{r}\right], \tag{10}$$

and

$$\sigma_t = \frac{E}{1 - v^2}\left[\frac{u}{r} + v\frac{\mathrm{d}u}{\mathrm{d}r} + v\frac{1}{2}\left(\frac{\mathrm{d}w}{\mathrm{d}r}\right)^2\right]. \tag{11}$$

Eliminating $\mathrm{d}u/\mathrm{d}r + (\mathrm{d}w/\mathrm{d}r)^2/2$ from Equations (10) and (11) and then eliminating σ_t using Equation (5) yields

$$\frac{u}{r} = \frac{1}{Eh}(\sigma_t h - v\sigma_r h) = \frac{1}{Eh}\left[\frac{\mathrm{d}}{\mathrm{d}r}(r\sigma_r h) - v\sigma_r h\right]. \tag{12}$$

The usually consistency equation can be finally written by eliminating u from Equations (10) and (12), as

$$r\frac{\mathrm{d}}{\mathrm{d}r}\left[\frac{1}{r}\frac{\mathrm{d}}{\mathrm{d}r}(r^2\sigma_r h)\right] + \frac{Eh}{2}\left(\frac{\mathrm{d}w}{\mathrm{d}r}\right)^2 = 0. \tag{13}$$

The specific solutions of the radial stress σ_r and deflection w can be obtained from Equations (4) and (13), where the boundary condition, under which Equations (4) and (13) can be solved, are

$$\frac{\mathrm{d}w}{\mathrm{d}r} = 0 \text{ at } r = 0, \tag{14}$$

$$\frac{u}{r} = \frac{1}{Eh}\left[\frac{\mathrm{d}}{\mathrm{d}r}(r\sigma_r h) - v\sigma_r h\right] = 0 \text{ at } r = a \tag{15}$$

and

$$w = 0 \text{ at } r = a. \tag{16}$$

Let us proceed to the following nondimensionalization

$$W = \frac{w}{a}, \ S_r = \frac{\sigma_r}{E}, \ S_t = \frac{\sigma_t}{E}, \ x = \frac{r}{a}, \ H_0 = \frac{H}{a}, \ G = \frac{\rho g a^2}{Eh}, \tag{17}$$

and transform Equations (4), (5), (13)–(16), respectively, into

$$4x^2 S_r^2 (-\frac{dW}{dx})^2 - G^2 [(-\frac{dW}{dx})^2 + 1][\int_0^x 2xW(x)dx + x^2 H_0]^2 = 0, \tag{18}$$

$$x^2 \frac{d^2 S_r}{dx^2} + 3x \frac{dS_r}{dx} + \frac{1}{2}(\frac{dW}{dx})^2 = 0, \tag{19}$$

$$S_t = S_r + x \frac{dS_r}{dx}, \tag{20}$$

$$\frac{dW}{dx} = 0 \text{ at } x = 0, \tag{21}$$

$$\frac{u}{r} = (1 - v)S_r + x \frac{dS_r}{dx} = 0 \text{ at } x = 1 \tag{22}$$

and

$$W = 0 \text{ at } x = 1. \tag{23}$$

S_r and W can be expanded into the power series of the x due to the fact that the stress and deflection are both finite at $x = 0$, i.e., letting

$$S_r = \sum_{i=0}^{\infty} c_i x^i \tag{24}$$

and

$$W = \sum_{i=0}^{\infty} d_i x^i. \tag{25}$$

The recursion formulas for the coefficients c_i and d_i in Equations (24) and (25) can be determined by substituting Equations (24) and (25) into Equations (17) and (18), and the results in this way are that both c_i and d_i are always equal to zero when i is odd and can be represented as the polynomials of c_0 and d_0 when i is even, as in Appendices A and B.

The remaining two coefficients, c_0 and d_0, are usually known as the undetermined constants, and they can be determined by using the boundary conditions at $x = 1$ as follows. From Equation (24), the boundary condition Equation (22) gives

$$(1 - v) \sum_{i=0}^{\infty} c_i + \sum_{i=1}^{\infty} i c_i = 0, \tag{26}$$

and from Equation (25), the boundary condition Equation (23) gives

$$\sum_{i=0}^{\infty} d_i = 0. \tag{27}$$

After substituting all the recursion formulas for the coefficients c_i and d_i into Equations (26) and (27) repeatedly, a system of equations containing only c_0 and d_0 can finally be obtained. As a result, the undetermined constants c_0 and d_0 can be determined by solving this system of equations, and with the known c_0 and d_0, the expressions of S_r and W can also be determined. The problem under consideration is thus solved analytically.

3. Results and Discussions

The boundary condition, Equation (21), which has not been used yet, i.e., the condition of $dW/dx = 0$ at $x = 0$, can be used to confirm the validity of the above analytical process.

The first derivative of the W versus the x can be obtained by the first derivative on both sides of Equation (25),

$$\frac{\mathrm{d}W}{\mathrm{d}x} = \sum_{i=1}^{\infty} id_i x^{i-1}. \tag{28}$$

Equation (28) shows that $\mathrm{d}W/\mathrm{d}x \equiv d_1$ when $x = 0$, while it can be seen from the derivation in Section 2 that $d_1 \equiv 0$ because $d_i \equiv 0$ when i is odd. Therefore, it may be concluded that $\mathrm{d}W/\mathrm{d}x \equiv 0$ at $x = 0$, which indicates that the boundary condition in Equation (21) can be naturally met by the closed-form solution obtained in Section 2. This to some extent indicates that the derivation in Section 2 is basically reliable.

3.1. The Convergence of the Power Series Solutions Obtained

Due to the complexity of the expressions of c_i and d_i (see Appendices A and B), the convergence of the power series solutions for radial stress and deflection obtained in Section 2 has to be discussed by examining the convergence of their specific solutions (rather than their general solutions). To this end, a numerical example was conducted where a peripherally fixed circular membrane with Poisson's ratio $v = 0.45$, Young's modulus of elasticity $E = 3.05$ MPa, thickness $h = 0.3$ mm and radius $a = 70$ mm was subjected to the weight of the liquid with density $\rho = 1 \times 10^{-6}$ kg/mm^3 and height $H = 300$ mm. For convenience, the infinite power series in Equations (26) and (27) have to be truncated to n terms, that is

$$(1-v)\sum_{i=0}^{n} c_i + \sum_{i=1}^{n} ic_i = 0 \tag{29}$$

and

$$\sum_{i=0}^{n} d_i = 0. \tag{30}$$

The value of the parameter n in Equations (29) and (30) should be specified firstly, and then all the recursion formulas for the coefficients c_i and d_i in Appendices A and B are repeatedly substituted into Equations (29) and (30) until a system of equations containing only the undetermined constants c_0 and d_0 can be finally obtained. The numerical values of c_0 and d_0, which correspond to the specified value of the parameter n, can be determined by solving this system of equations with regard to c_0 and d_0.

We began the numerical value calculations of c_0 and d_0 from $n = 2$; the calculation results are listed in Table 1 and the variations of c_0 and d_0 with n are shown in Figures 3 and 4. From Figures 3 and 4, it may be seen that the data sequences of c_0 and d_0 already converge well when $n = 18$. Therefore, only the recursion formulas for the coefficients c_i and d_i when $i \leq 20$ are listed in Appendices A and B, and the undetermined constants c_0 and d_0 can finally take $1.98216876 \times 10^{-1}$ and $3.91482802 \times 10^{-1}$, respectively, i.e., the values at $n = 20$ in Table 1.

Table 1. Numerical values of c_0 and d_0 at different n when $H = 300$ mm.

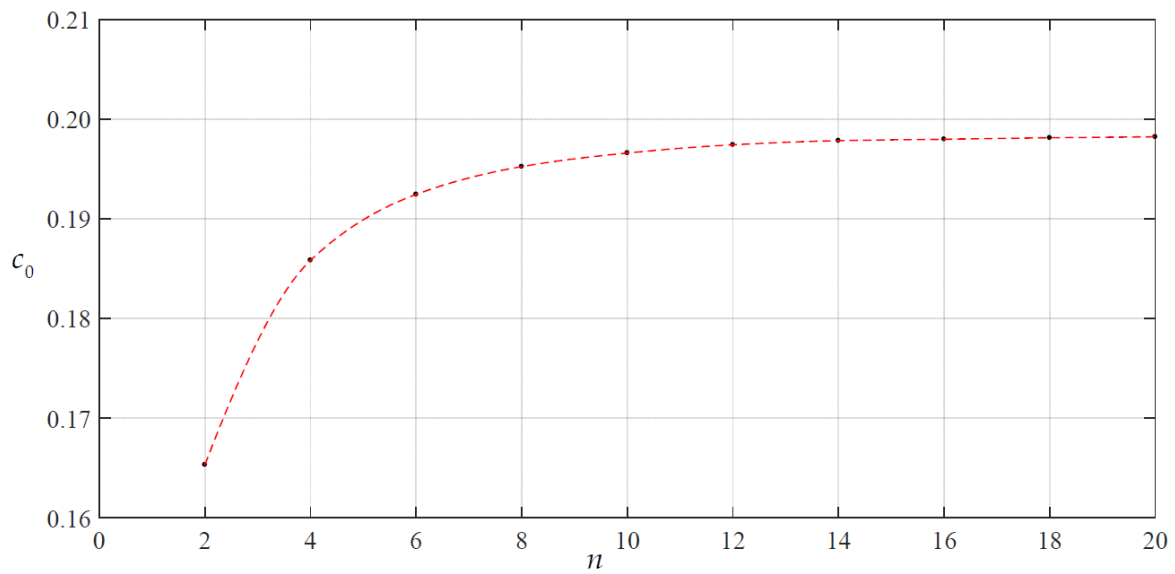| n	c_0	d_0
2	$1.65316391 \times 10^{-1}$	$3.77658452 \times 10^{-1}$
4	$1.85832249 \times 10^{-1}$	$3.95315235 \times 10^{-1}$
6	$1.92438471 \times 10^{-1}$	$3.95548206 \times 10^{-1}$
8	$1.95231453 \times 10^{-1}$	$3.94159221 \times 10^{-1}$
10	$1.96595308 \times 10^{-1}$	$3.93001167 \times 10^{-1}$
12	$1.97422893 \times 10^{-1}$	$3.92241509 \times 10^{-1}$
14	$1.97834610 \times 10^{-1}$	$3.91803156 \times 10^{-1}$
16	$1.97977443 \times 10^{-1}$	$3.91614348 \times 10^{-1}$
18	$1.98125067 \times 10^{-1}$	$3.91540206 \times 10^{-1}$
20	$1.98216876 \times 10^{-1}$	$3.91482802 \times 10^{-1}$

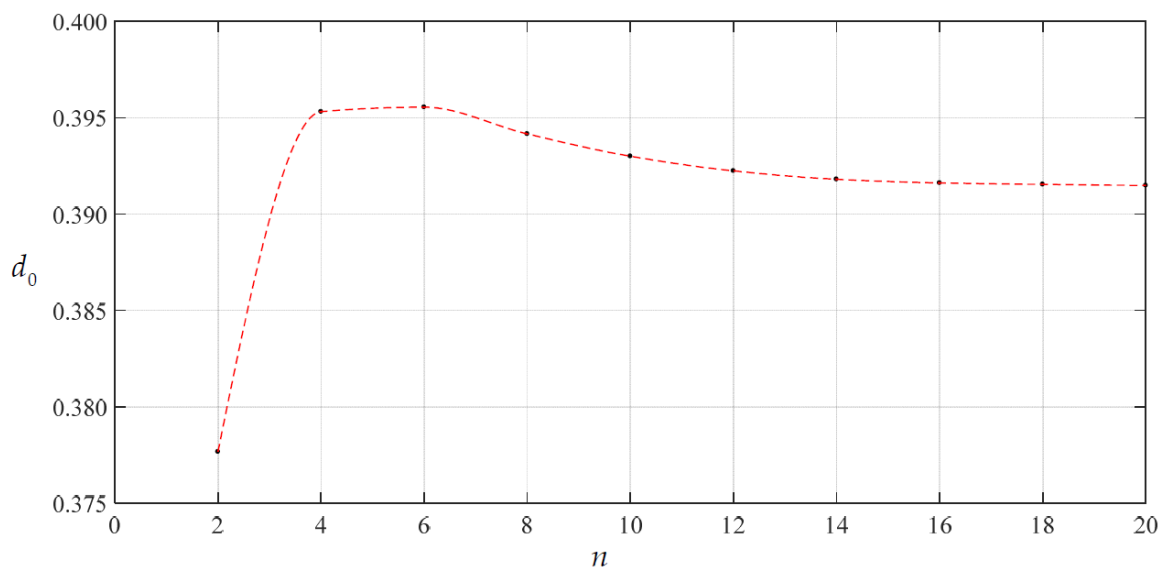**Figure 3.** Variation of c_0 with n when H = 300 mm.

Figure 4. Variation of d_0 with n when H = 300 mm.

To examine the convergence of the special solutions of stress and deflection with $c_0 = 1.98216876 \times 10^{-1}$ and $d_0 = 3.91482802 \times 10^{-1}$ the numerical values of c_i and d_i were calculated, as listed in Table 2. The variations of c_i and d_i with i are shown in Figures 5 and 6. It may be seen from Figures 5 and 6 that the special solutions of stress and deflection at $x = 1$ (i.e., at $r = a = 70$ mm, the worst case) converge very well.

Table 2. Numerical values of c_i and d_i when $c_0 = 1.98216876 \times 10^{-1}$, $d_0 = 3.91482802 \times 10^{-1}$ and $H = 300$ mm.

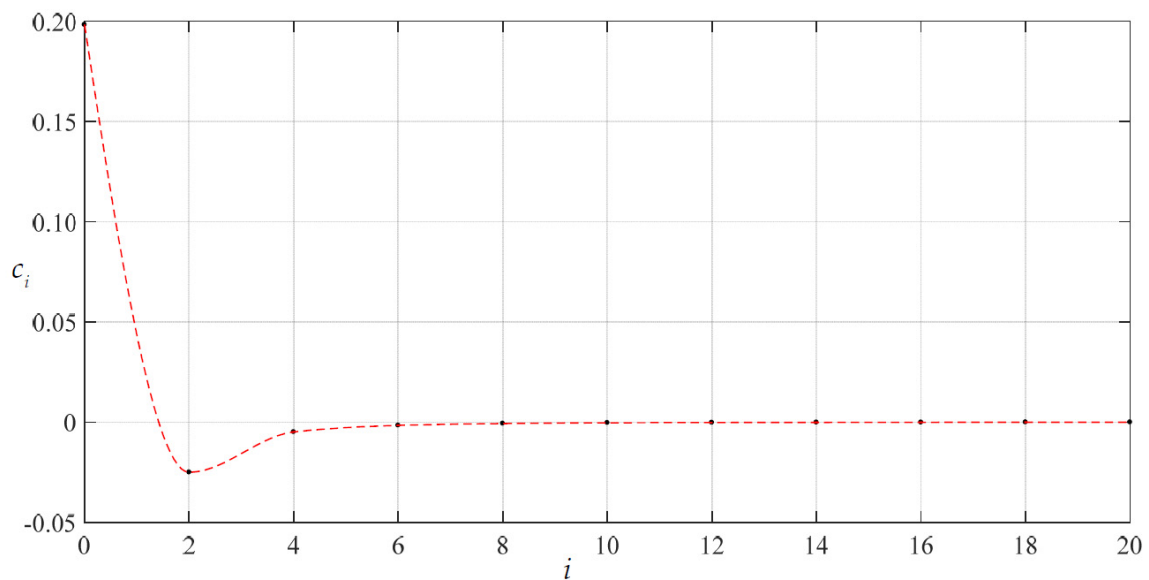| i	c_i	d_i
0	$1.98216876 \times 10^{-1}$	$3.91482802 \times 10^{-1}$
2	$-2.49493987 \times 10^{-2}$	$-3.15907573 \times 10^{-1}$
4	$-4.85171579 \times 10^{-3}$	$-4.60740692 \times 10^{-2}$
6	$-1.58206170 \times 10^{-3}$	$-1.55521234 \times 10^{-2}$
8	$-6.42288769 \times 10^{-4}$	$-6.76343212 \times 10^{-3}$
10	$-2.94655565 \times 10^{-4}$	$-3.32901660 \times 10^{-3}$
12	$-1.46220841 \times 10^{-4}$	$-1.76487967 \times 10^{-3}$
14	$-7.66573427 \times 10^{-5}$	$-9.83324535 \times 10^{-4}$
16	$-4.18541507 \times 10^{-5}$	$-5.67748867 \times 10^{-4}$
18	$-2.35781462 \times 10^{-5}$	$-3.36715864 \times 10^{-4}$
20	$-1.36166630 \times 10^{-5}$	$-2.03918152 \times 10^{-4}$

Figure 5. Variation of c_i with i when $c_0 = 1.98216876 \times 10^{-1}$, $d_0 = 3.91482802 \times 10^{-1}$ and $H = 300$ mm.
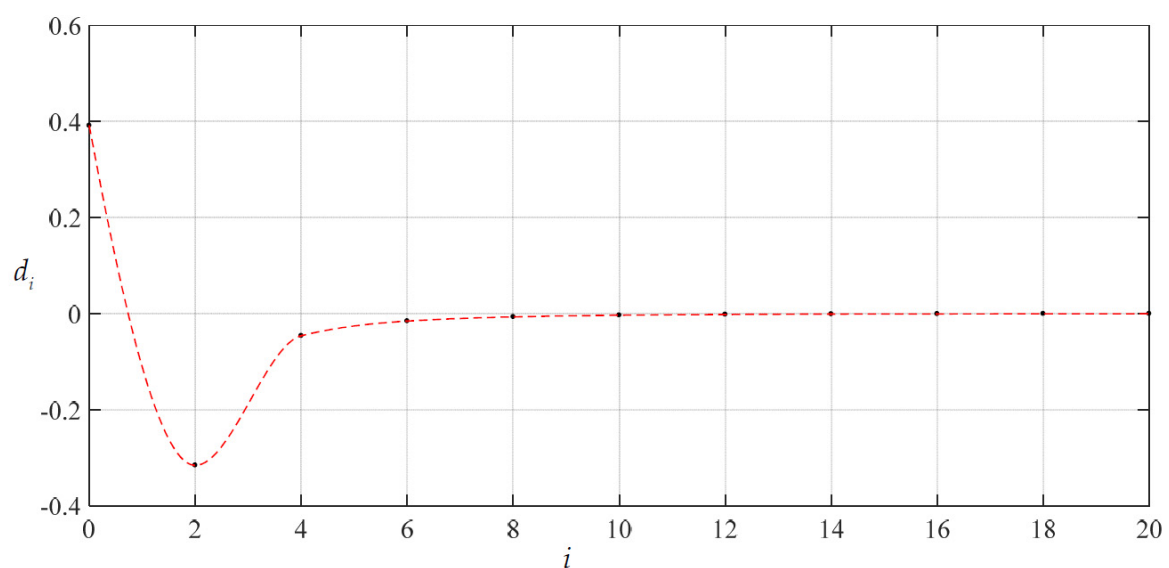

Figure 6. Variation of d_i with i when $c_0 = 1.98216876 \times 10^{-1}$, $d_0 = 3.91482802 \times 10^{-1}$ and $H = 300$ mm.

3.2. The Improved Effect of the Integro-Differential Out-of-Plane Equilibrium Equation

In Section 2, the approximation of replacing $\sin\theta = 1/(1 + 1/\tan^2\theta)^{1/2}$ with $\sin\theta = \tan\theta$ has been discarded during the derivation of the integro-differential equation for governing the out-of-plane equilibrium. Now, let us see the effect of giving up this approximation on the closed-form solutions. Figures 7 and 8 show the variation of deflection and stress along the diameter when the height H of the rainwater stored in the container reaches 10, 300 and 1000 mm, respectively. In Figures 7 and 8, Solution 1 refers to the closed-form solution, which is obtained by using $\sin\theta = 1/(1 + 1/\tan^2\theta)^{1/2}$ in Section 2, while Solution 2 refers to the closed-form solution which is obtained by using $\sin\theta = \tan\theta$ in [5]. Therefore, the comparison between Solution 1 and Solution 2 can reflect the effect of giving up the approximation of replacing $\sin\theta = 1/(1 + 1/\tan^2\theta)^{1/2}$ with $\sin\theta = \tan\theta$. It may be seen from Figures 7 and 8 that the two solutions agree quite closely when the height H of the rainwater in the storage container is relatively small, but as the height H increases they gradually diverge. This means that the use of $\sin\theta = 1/(1 + 1/\tan^2\theta)^{1/2}$ in Solution 1 has a noticeable effect.
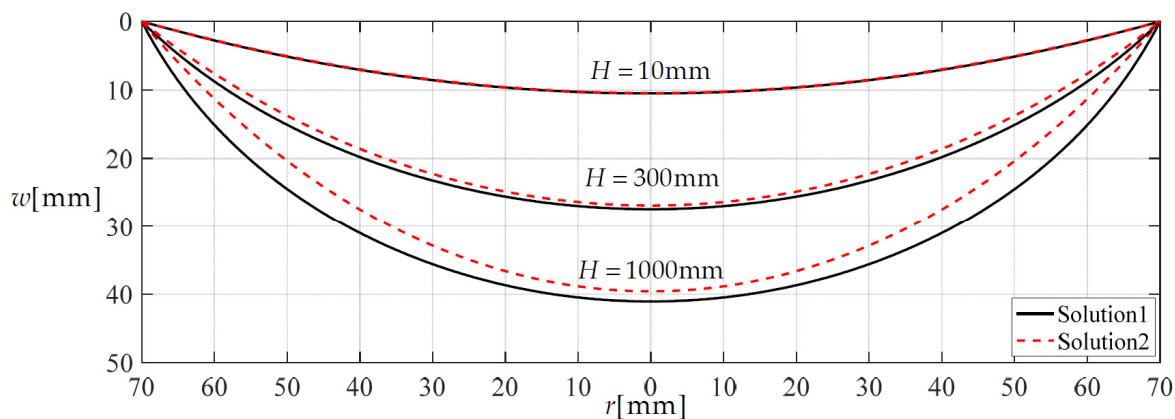

Figure 7. The variations of w with r when H takes 10, 300 and 1000 mm, respectively.
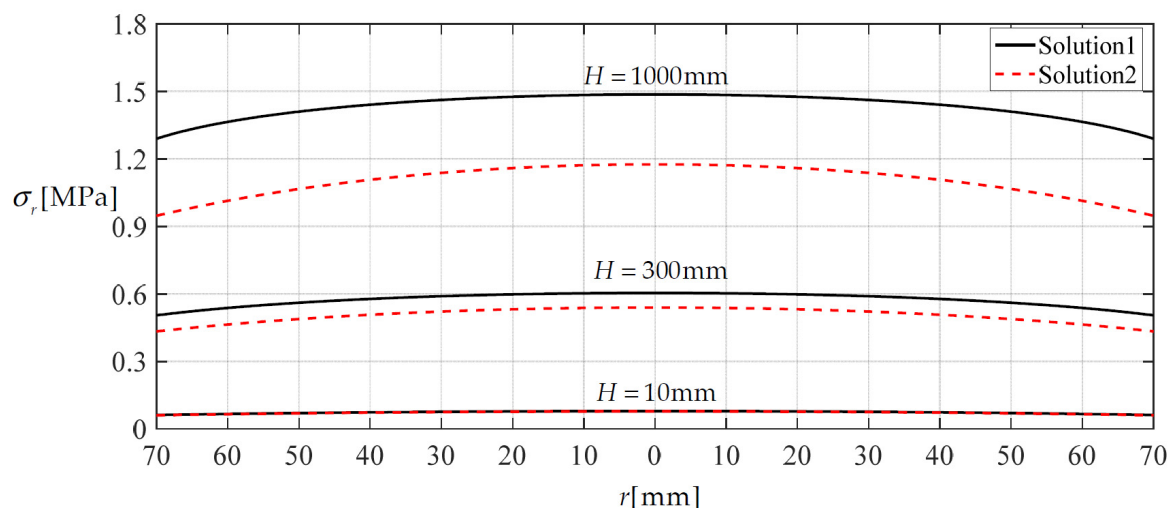
Figure 8. Variations of σ_r with r when H is 10, 300 and 1000 mm, respectively.

3.3. Two Typical Applications of the Closed-form Solution Given

The membrane deflection-based rain gauges to be developed will involve two main types: one directly measures the maximum deflection w_m of the deflected circular membrane, as shown in Figure 1, and the other is to measure the capacitance of the non-parallel plate capacitor as shown in Figure 9. The first type of rain gauge can use any thin film with

good elasticity as the elastic bottom of the rainwater storage container, while the second type must use conductive thin films [30,31] with both good elasticity and good electrical conductivity as the upper electrode plate of the non-parallel plate capacitor (see Figure 9). Let us continue with the numerical examples conducted in Section 3.1 to illustrate the application of the closed-form solution given in Section 2 in designing such membrane deflection-based rain gauges. We present here only the numerical calibration of such rain gauges based on the closed-form solution given in Section 2.
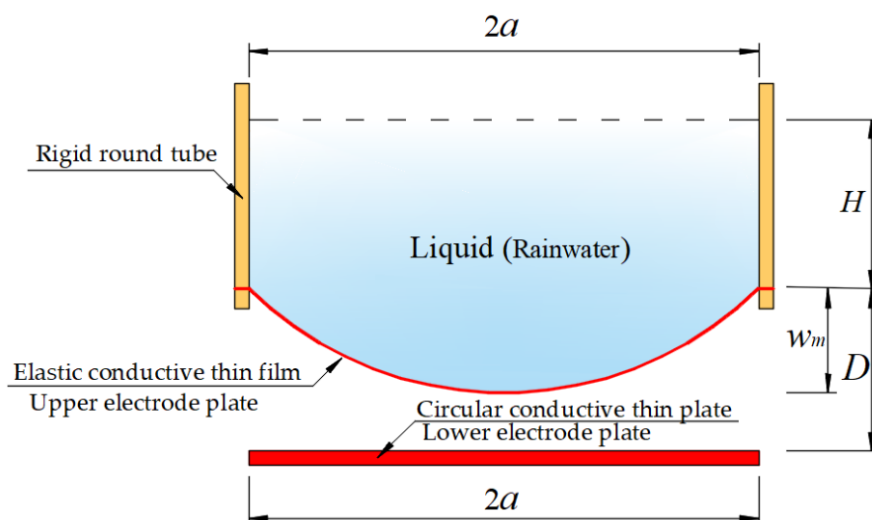

Figure 9. Sketch of rain gauges based on membrane deflection and non-parallel plate capacitor.

For the first type of rain gauge, the maximum deflection w_m of the deflected circular membrane can be directly measured, for example, by a non-contact laser displacement sensor. Figure 10 shows a scatter diagram describing the relationship between the height H of the rainwater in the storage container and the maximum deflection w_m of the deflected circular membrane, where the values of the scatter points are calculated using the closed-form solution given in Section 2, and then to fit the curve $H = 44.34 - 11.23\,w_\mathrm{m} + 0.7323\,w_\mathrm{m}^2$. Therefore, with the measured values of the maximum deflection w_m, the corresponding values of the height H of the rainwater in the storage container can be determined using the analytical expression $H = 44.34 - 11.23\,w_\mathrm{m} + 0.7323\,w_\mathrm{m}^2$.

As for the second type of rain gauge shown in Figure 9, the capacitance of the non-parallel plate capacitor is given by [13,32].

$$C = \varepsilon_0 \varepsilon_r \int_0^{2\pi} \int_0^a \frac{r}{D - w(r,\varphi)}\,\mathrm{d}\varphi\,\mathrm{d}r = 2\pi\varepsilon_0 \varepsilon_r \int_0^a \frac{r}{D - w(r)}\,\mathrm{d}r, \tag{31}$$

where ε_0 is the vacuum dielectric constant ($\varepsilon_0 = 8.854187817 \times 10^{-12}$ F/m), ε_r is the relative permittivity of dry air ($\varepsilon_r = 1.000585$), and D is the initial gap between the initial flat circular membrane and the circular conductive thin plate (suppose that D takes 35 mm here). From Equations (17) and (25) the dimensional deflection $w(r)$ can be written as

$$w(r) = \sum_{i=0}^{\infty} \frac{d_i}{a^{i-1}} r^i. \tag{32}$$

If letting

$$\frac{r}{D - w(r)} = \sum_{i=0}^{\infty} b_i r^i, \tag{33}$$

then it is not difficult that the coefficients b_i is expressed as the polynomials with regards to d_i and D. Therefore, the capacitance of the non-parallel plate capacitor as shown in Figure 9 can be finally written as

$$C = 2\pi\varepsilon_0\varepsilon_r \int_0^a \left(\sum_{i=0}^{\infty} b_i r^i\right)dr = 2\pi\varepsilon_0\varepsilon_r \sum_{i=0}^{\infty} \frac{b_i a^{i+1}}{i+1}, \tag{34}$$

where $b_i \equiv 0$ ($i = 0, 2, 4, \dots$) and b_i ($i = 1, 3, 5, \dots$) are listed in Appendix C.
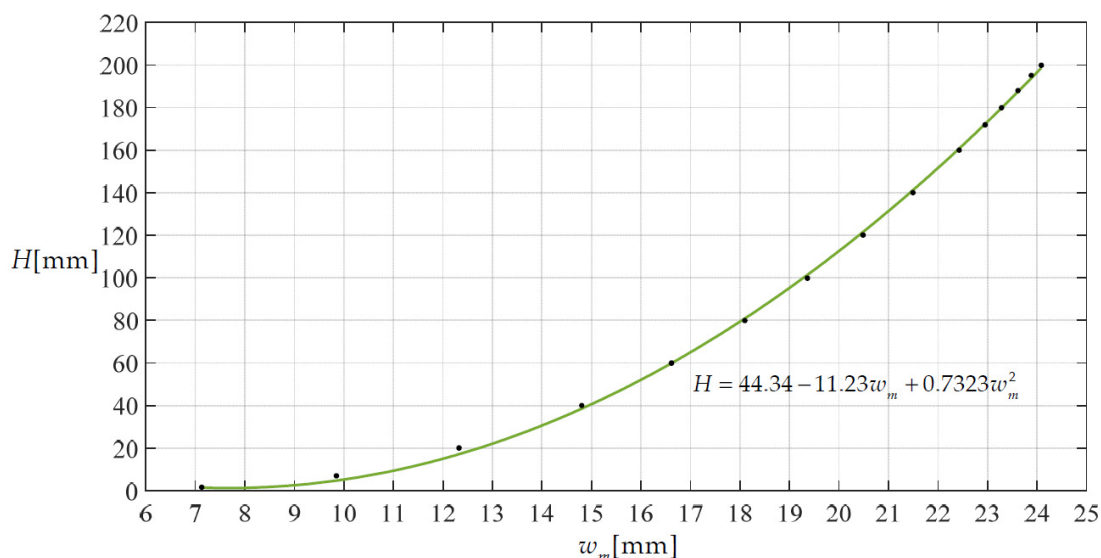

Figure 10. A scatter diagram describing the relationship of height H and maximum deflection w_m.

Figure 11 shows a scatter diagram describing the relationship between the height H of the rainwater in the storage container and the capacitance C of the non-parallel plate capacitor, where the values of the scatter points are calculated using the closed-form solution given in Section 2 and Equation (34), and then used to fit the curve $H = (0.3596C^2 + 197.6C - 877.2)/(C - 2.09)$. Therefore, with the measured values of the capacitance C, the corresponding values of the height H of the rainwater in the storage container can be determined using the analytical expression $H = (0.3596C^2 + 197.6C - 877.2)/(C - 2.09)$.
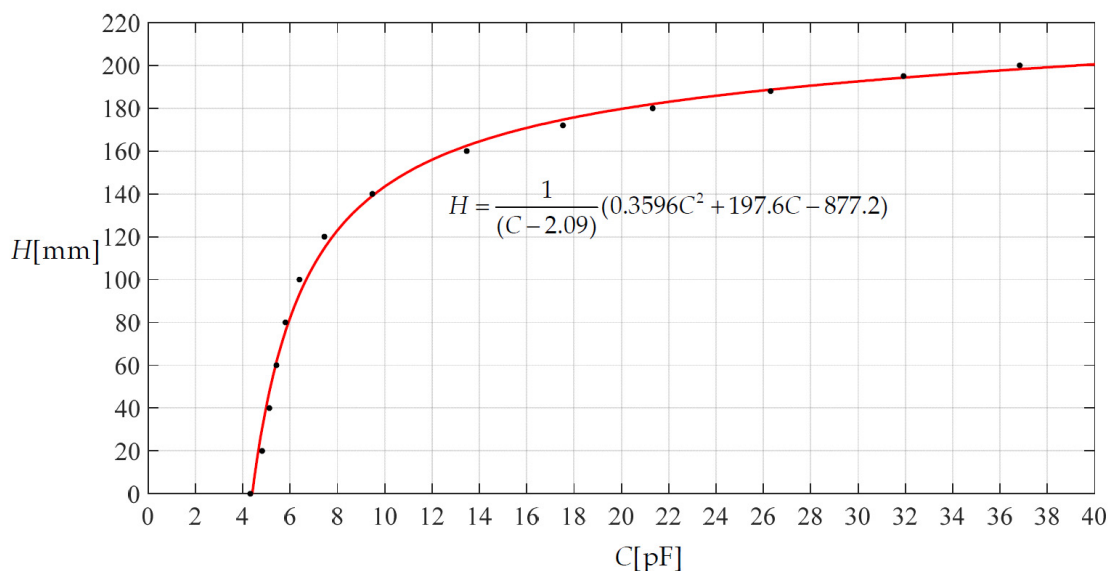

Figure 11. A scatter diagram describing the relationship of height H and capacitance C.

3.4. Confirmatory Experiment

In order to verify the validity of the closed-form solution given in Section 2, we conducted a confirmatory experiment. As shown in Figure 12, a peripherally fixed circular silicon rubber thin-film with Poisson's ratio $v = 0.45$, Young's modulus of elasticity $E = 3.05$ MPa, thickness $h = 2$ mm and radius $a = 70$ mm was subjected to the weight of the liquid (colored water) with density $\rho = 1 \times 10^{-6}$ kg/mm^3 and height $H = 100$ mm. We use a non-contact laser displacement sensor (ZSY Group Ltd., London, UK, see Figure 12c) to measure membrane deflection at 13 test points (see Figure 12d). The results of the experimental test and theoretical calculation of deflection as well as their relative errors are listed in Table 3, and the deflection curves along the diameter are shown in Figure 13.
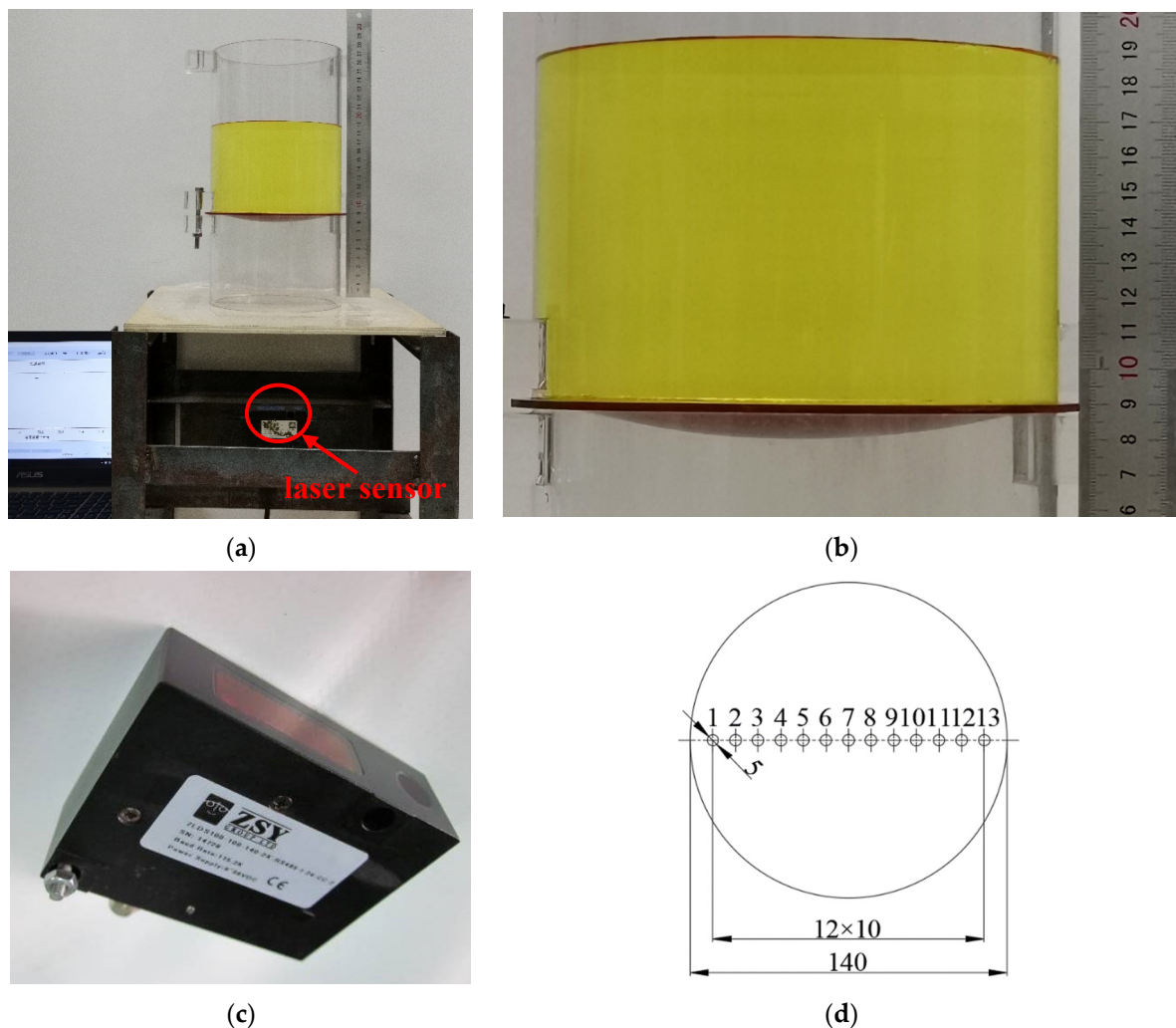

Figure 12. Confirmatory experiment: (**a**) experimental setup; (**b**) a detailed view of the colored water part (**a**); (**c**) laser displacement sensor; (**d**) positions of 13 test points.

Table 3. Experimental and theoretical values of deflection and their relative errors when H = 97.5 mm.

Test Points	Radius	Experimental Results	Calculated Results	Relative Errors
1	60	2.89	2.8400	1.73%
2	50	5.19	5.1016	1.70%
3	40	6.99	6.8729	1.67%
4	30	8.33	8.2082	1.46%
5	20	9.27	9.1414	1.39%
6	10	9.80	9.6937	1.08%
7	0	9.97	9.8766	0.94%
8	10	9.82	9.6937	1.29%
9	20	9.29	9.1414	1.60%
10	30	8.34	8.2082	1.58%
11	40	6.96	6.8729	1.25%
12	50	5.19	5.1016	1.70%
13	60	2.89	2.8400	1.73%

Relative errors = |Experimental results–Theoretical results|/Experimental results.
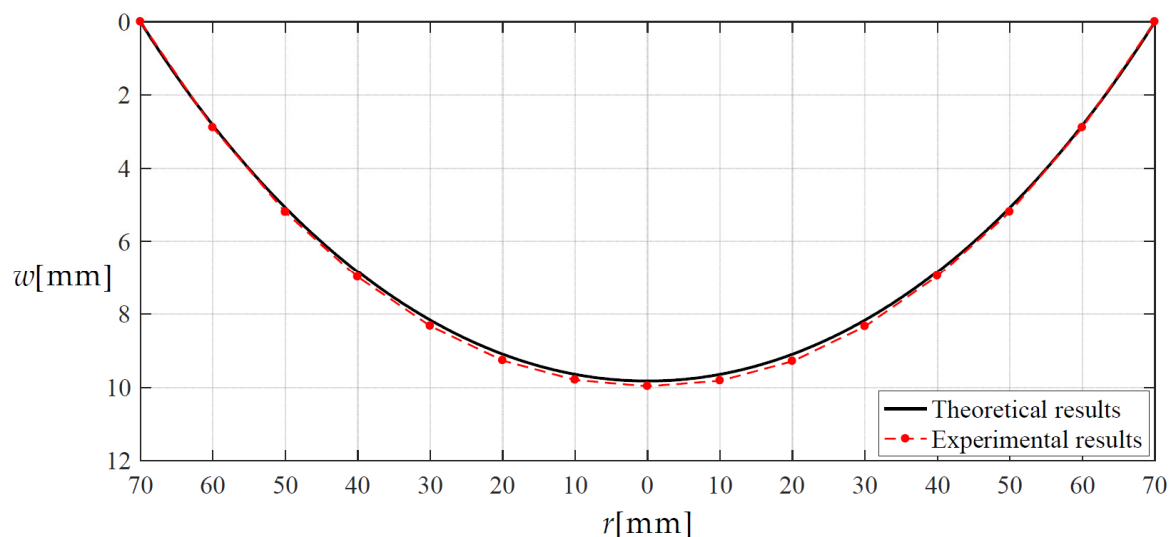
Figure 13. Membrane deflection along the diameter when H = 97.5 mm.

It may be seen from Table 3 or Figure 13 that the results of experimental test and theoretical calculation agree well, which means that the closed-form solution obtained in Section 2 is basically reliable. Of course, the computational accuracy of the closed-form solution presented here needs to be further improved. Some approximations or assumptions are still used during the derivation of the in-plane equilibrium and geometric equations, which should be the main reason for the relative errors in Table 3.

4. Concluding Remarks

In this paper, the statics problem of the fluid–structure interaction of a peripherally fixed circular membrane subjected to liquid weight loading is reformulated, where the approximation of replacing $\sin\theta = 1/(1 + 1/\tan^2\theta)^{1/2}$ with $\sin\theta = \tan\theta$, which is adopted in the earlier work [5], is discarded. The previous integro-differential equation governing the out-of-plane equilibrium, established by using $\sin\theta = \tan\theta$ in [5], was modified using $\sin\theta = 1/(1 + 1/\tan^2\theta)^{1/2}$, resulting in a new and more complicated integro-differential equation governing the out-of-plane equilibrium. The reformulated problem was solved using the power series method, and a new and more refined closed-form solution of the problem was finally given. Some important issues were addressed numerically and experimentally. The following conclusions can be drawn from this study.

The sine function, $\sin\theta$, can be approximated by the tangent function, $\tan\theta$, only when the rotation angle θ of membrane is relatively small; when the rotation angle θ of membrane is relatively large, such an approximation will give rise to a significant error. For instance, the error caused by using $\tan\theta$ to approximate $\sin\theta$ was about 1.54% when $\theta = 10°$, 6.42% when $\theta = 20°$, 15.47% when $\theta = 30°$, and 30.54% when $\theta = 40°$. In fact, the rotation-angle θ of the membrane may exceed $40°$ for membrane deflection-based rain gauges to be developed. Therefore, it is necessary and worthwhile for such technical applications to discard the approximation of replacing $\sin\theta = 1/(1 + 1/\tan^2\theta)^{1/2}$ with $\sin\theta = \tan\theta$ during the derivation of the closed-form solution of the problem under consideration.

The power series method is a very effective mathematical tool for solving nonlinear equations. Although the new integro-differential equation governing the out-of-plane equilibrium is much more complicated than the previous one, the power series solutions obtained for stress and deflection still have good convergence and fast convergence speed.

In addition, the closed-form solution obtained in Section 2 is in good agreement with the confirmatory experiment conducted, suggesting that this closed-form solution is basically reliable and can be used to design the membrane deflection-based rain gauges to be developed.

Institutional Review Board Statement: Not applicable.

Informed Consent Statement: Not applicable.

Data Availability Statement: Not applicable.

Conflicts of Interest: The authors declare no conflict of interest.

Nomenclature

a	Radius of the circular membrane
h	Thickness of the circular membrane
E	Young's modulus of elasticity
ν	Poisson's ratio
H	Height of the liquid in the storage container
ρ	Density of the liquid in the storage container
g	Acceleration of gravity
r	Radial coordinate of the cylindrical coordinate system (r, φ, w)
φ	Circumferential angle coordinate of (r, φ, w)
w	Axial coordinate of (r, φ, w) as well as transverse displacement
u	Radial displacement of the deflected circular membrane
w_{m}	Maximum deflection of the deflected circular membrane
$q(r)$	Transverse loads that varies continuously with the radial coordinate r
$F(r)$	External force produced by $q(r)$ within radius r
σ_r	Radial stress
σ_t	Circumferential stress
e_r	Radial strain
e_t	Circumferential strain
θ	Rotation angle of the deflected circular membrane
π	Pi (ratio of circumference to diameter)
W	Dimensionless transverse displacement (w/a)

S_r Dimensionless radial stress (σ_r/E)

S_t Dimensionless circumferential stress (σ_t/E)

H_0 Dimensionless height H (H/a)

G Dimensionless quantity ($\rho g a^2/Eh$)

x Dimensionless radial coordinate (r/a)

C Capacitance of a non-parallel plate capacitor

D Initial gap of the non-parallel plate capacitor

b_i Coefficients of the power series for capacitance C

c_i Coefficients of the power series for S_r

d_i Coefficients of the power series for W

Appendix A

$$c_2 = -\frac{G^2(H_0 + d_0)^2}{64 c_0^2},$$

$$c_4 = -\frac{1}{192\,c_0^2}(4\,G^2H_0^2d_2^2 + 8\,G^2H_0d_0d_2^2 + 4\,G^2d_0^2d_2^2 + G^2H_0d_2 + G^2d_0d_2 - 32\,c_0c_2d_2^2),$$

$$
\begin{aligned}
c_6 = -\frac{1}{4608\,c_0^2}\big(&192\,G^2H_0^2d_2d_4 + 384\,G^2H_0d_0d_2d_4 + 48\,G^2H_0d_2^3 + 192\,G^2d_0^2d_2d_4 + 48\,G^2d_0d_2^3 \\
&+ 8\,G^2H_0d_4 + 8\,G^2d_4d_0 + 3\,G^2d_2^2 - 1536\,c_0c_2d_2d_4 - 384\,c_0c_4d_2^2 - 192\,c_2^2d_2^2\big)
\end{aligned}
$$

$$
\begin{aligned}
c_8 = -\frac{1}{3840\,c_0^2}\big(&144\,G^2H_0^2d_2d_6 + 96\,G^2H_0^2d_4^2 + 288\,G^2H_0d_0d_2d_6 + 192\,G^2H_0d_0d_4^2 + 96\,G^2d_0^2d_4^2 \\
&+ 112\,G^2H_0d_2^2d_4 + 144\,G^2d_0^2d_2d_6 + 112\,G^2d_0d_0^2d_4 + 6\,G^2d_2^4 + 3\,G^2H_0d_6 - 768\,c_0c_4d_2d_4 \\
&+ 3\,G^2d_6d_0 + 2\,G^2d_4d_2 - 1152\,c_0c_2d_2d_6 - 768\,c_0c_2d_4^2 - 192\,c_0c_6d_2^2 - 384\,c_2^2d_2d_4 - 192\,c_2c_4d_2^2\big)
\end{aligned}
$$

$$
\begin{aligned}
c_{10} = -\frac{1}{172800c_0^2}\big(&5760G^2H_0^2d_2d_8 + 8640G^2H_0^2d_4d_6 + 11520G^2H_0d_0d_2d_8 + 17280G^2H_0d_0d_4d_6 \\
&+ 4680G^2H_0d_2^2d_6 + 4800G^2H_0d_2d_4^2 + 5760G^2d_0^2d_2d_8 + 8640G^2d_0^2d_4d_6 + 4680G^2d_0d_2^2d_6 \\
&+ 4800G^2d_0d_2d_4^2 + 960G^2d_2^3d_4 + 72G^2H_0d_8 + 72G^2d_0d_8 + 45G^2d_2d_6 + 20G^2d_4^2 \\
&- 46080c_0c_2d_2d_8 - 69120c_0c_2d_4d_6 - 34560c_0c_4d_2d_6 - 23040c_0c_4d_4^2 - 23040c_0c_6d_2d_4 \\
&- 5760c_0c_8d_2^2 - 17280c_2^2d_2d_6 - 11520c_2^2d_4^2 - 23040c_2c_4d_2d_4 - 5760c_2c_6d_2^2 - 2880c_4^2d_2^2\big)
\end{aligned}
$$

$$
\begin{aligned}
c_{12} = -\frac{1}{120960c_0^2}\big(&3600G^2H_0^2d_2d_{10} + 5760G^2H_0^2d_4d_8 + 3240G^2H_0^2d_6^2 + 7200G^2H_0d_0d_2d_{10} \\
&+ 11520G^2H_0d_0d_4d_8 + 6480G^2H_0d_0d_6^2 + 3024G^2H_0d_2^2d_8 + 6480G^2H_0d_2d_4d_6 + 960G^2H_0d_4^3 \\
&+ 3600G^2d_0^2d_2d_{10} + 5760G^2d_0^2d_4d_8 + 3240G^2d_0^2d_6^2 + 3024G^2d_0d_2^2d_8 + 6480G^2d_0d_2d_4d_6 \\
&+ 960G^2d_0d_4^3 + 630G^2d_2^3d_6 - 46080c_0c_2d_4d_8 + 30G^2H_0d_{10} + 30G^2d_0d_{10} + 18G^2d_2d_8 \\
&+ 15G^2d_4d_6 - 28800c_0c_2d_2d_{10} + 880G^2d_2^2d_4^2 - 25920c_0c_2d_6^2 - 23040c_0c_4d_2d_8 - 34560c_0c_4d_4d_6 \\
&- 17280c_0c_6d_2d_6 - 11520c_0c_6d_4^2 - 11520c_0c_8d_2d_4 - 2880c_0c_{10}d_2^2 - 11520c_2^2d_2d_8 - 17280c_2^2d_4d_6 \\
&- 17280c_2c_4d_2d_6 - 11520c_2c_4d_4^2 - 11520c_0c_6d_2d_4 - 2880c_2c_8d_2^2 - 5760c_4^2d_2d_4 - 2880c_4c_6d_2^2\big)
\end{aligned}
$$

$$
\begin{aligned}
c_{14} = -\frac{1}{9031680c_0^2}\big(&241920G^2H_0^2d_2d_{12} + 403200G^2H_0^2d_4d_{10} + 483840G^2H_0^2d_6d_8 - 322560c_4^2d_4^2 \\
&+ 483840G^2H_0d_0d_2d_{12} + 806400G^2H_0d_0d_4d_{10} + 967680G^2H_0d_0d_6d_8 + 208320G^2H_0d_2^2d_{10} \\
&+ 462336G^2H_0d_2d_4d_8 + 241920G^2H_0d_2d_6^2 + 201600G^2H_0d_4^2d_6 + 241920G^2d_0^2d_2d_{12} \\
&+ 403200G^2d_0^2d_4d_{10} + 483840G^2d_0^2d_6d_8 + 208320G^2d_0d_2^2d_{10} + 462336G^2d_0d_2d_4d_8 \\
&+ 241920G^2d_0d_2d_6^2 + 201600G^2d_0d_4^2d_6 + 44352G^2d_2^3d_8 + 124320G^2d_2^2d_4d_6 + 35840G^2d_2d_4^3 \\
&+ 1440G^2H_0d_{12} + 1440G^2d_0d_{12} + 840G^2d_2d_{10} + 672G^2d_4d_8 + 315G^2d_6^2 - 1935360c_0c_2d_2d_{12} \\
&- 3225600c_0c_2d_4d_{10} - 3870720c_0c_2d_6d_8 - 1612800c_0c_4d_2d_{10} - 2580480c_0c_4d_4d_8 \\
&- 1451520c_0c_4d_6^2 - 1290240c_0c_6d_2d_8 - 1935360c_0c_6d_4d_6 - 967680c_0c_8d_2d_6 - 645120c_0c_8d_4^2 \\
&- 645120c_0c_{10}d_2d_4 - 161280c_0c_{12}d_2^2 - 806400c_2^2d_2d_{10} - 1290240c_2^2d_4d_8 - 725760c_2^2d_6^2 \\
&- 1290240c_2c_4d_2d_8 - 1935360c_2c_4d_4d_6 - 967680c_2c_6d_2d_6 - 645120c_2c_6d_4^2 - 645120c_2c_8d_2d_4 \\
&- 161280c_2c_{10}d_2^2 - 483840c_4^2d_2d_6 - 645120c_4c_6d_2d_4 - 161280c_4c_8d_2^2 - 80640c_6^2d_2^2\big)
\end{aligned}
$$

$$c_{16} = -\frac{1}{2903040c_0^2}(70560G^2H_0^2d_2d_{14} + 120960G^2H_0^2d_4d_{12} + 151200G^2H_0^2d_6d_{10} + 80640G^2H_0^2d_8^2$$
$$+141120G^2H_0d_0d_2d_{14} + 241920G^2H_0d_0d_4d_{12} + 302400G^2H_0d_0d_6d_{10} + 161280G^2H_0d_0d_8^2$$
$$+61920G^2H_0d_2^2d_{12} + 141120G^2H_0d_2d_4d_{10} + 153216G^2H_0d_2d_6d_8 + 61824G^2H_0d_4^2d_8$$
$$+60480G^2H_0d_4d_6^2 + 70560G^2d_0^2d_2d_{14} + 120960G^2d_0^2d_4d_{12} + 151200G^2d_0^2d_6d_{10}$$
$$+80640G^2d_0^2d_8^2 + 61920G^2d_0d_2^2d_{12} + 141120G^2d_0d_2d_4d_{10} + 153216G^2d_0d_2d_6d_8$$
$$+61824G^2d_0d_4^2d_8 + 60480G^2d_0d_4d_6^2 + 13440G^2d_2^3d_{10} + 38304G^2d_2^2d_4d_8 + 140G^2d_4d_{10}$$
$$+19215G^2d_2^2d_6^2 + 31920G^2d_2d_4^2d_6 + 2240G^2d_4^4 + 315G^2H_0d_{14} + 315G^2d_0d_{14} + 180G^2d_2d_{12}$$
$$+126G^2d_6d_8 - 564480c_0c_2d_2d_{14} - 967680c_0c_2d_4d_{12} - 1209600c_0c_2d_6d_{10} - 645120c_0c_2d_8^2$$
$$-806400c_0c_4d_4d_{10} - 967680c_0c_4d_6d_8 - 403200c_0c_6d_2d_{10} - 645120c_0c_6d_4d_8 - 483840c_0c_4d_2d_{12}$$
$$-362880c_0c_6d_6^2 - 322560c_0c_8d_2d_8 - 483840c_0c_8d_4d_6 - 241920c_0c_{10}d_2d_6 - 161280c_0c_{10}d_4^2$$
$$-161280c_0c_{12}d_2d_4 - 40320c_0c_{14}d_2^2 - 241920c_2^2d_2d_{12} - 403200c_2^2d_4d_{10} - 483840c_2^2d_6d_8$$
$$-403200c_2c_4d_2d_{10} - 645120c_2c_4d_4d_8 - 362880c_2c_4d_6^2 - 322560c_2c_6d_2d_8 - 483840c_2c_6d_4d_6$$
$$-241920c_2c_8d_2d_6 - 161280c_2c_8d_4^2 - 161280c_2c_{10}d_2d_4 - 40320c_2c_{12}d_2^2 - 161280c_4^2d_2d_8$$
$$-241920c_4^2d_4d_6 - 241920c_4c_6d_2d_6 - 161280c_4c_6d_4^2 - 161280c_4c_8d_2d_4 - 40320c_4c_{10}d_2^2$$
$$-80640c_6^2d_2d_4 - 40320c_6c_8d_2^2)$$

$$c_{18} = -\frac{1}{36288000c_0^2}(806400G^2H_0^2d_2d_{16} + 1411200G^2H_0^2d_4d_{14} + 1814400G^2H_0^2d_6d_{12}$$
$$+2016000G^2H_0^2d_8d_{10} + 1612800G^2H_0d_0d_2d_{16} + 2822400G^2H_0d_0d_4d_{14} + 718200d_2^2G^2d_{14}H_0$$
$$+4032000G^2H_0d_0d_8d_{10} + 3628800G^2H_0d_0d_6d_{12} + 1670400G^2H_0d_2d_4d_{12} + 967680G^2H_0d_2d_8^2$$
$$+1864800G^2H_0d_2d_6d_{10} + 739200G^2H_0d_4^2d_{10} + 1451520G^2H_0d_4d_6d_8 + 226800G^2H_0d_6^3$$
$$+806400G^2d_0^2d_2d_{16} + 1411200G^2d_0^2d_4d_{14} + 1814400G^2d_0^2d_6d_{12} + 2016000G^2d_0^2d_8d_{10}$$
$$+718200d_2^2G^2d_{14}d_0 + 1670400G^2d_0d_2d_4d_{12} + 1864800G^2d_0d_2d_6d_{10} + 967680G^2d_0d_2d_8^2$$
$$+739200G^2d_0d_4^2d_{10} + 1451520G^2d_0d_4d_6d_8 + 226800G^2d_0d_6^3 + 158400G^2d_2^3d_{12} + 1050G^2d_6d_{10}$$
$$+459200G^2d_2^2d_4d_{10} + 468720G^2d_2^2d_6d_8 + 380800G^2d_2d_4^2d_8 + 365400G^2d_2d_4d_6^2 + 504G^2d_8^2$$
$$+100800G^2d_4^3d_6 + 2800G^2d_{16}H_0 + 2800G^2d_{16}d_0 + 1575G^2d_2d_{14} + 1200G^2d_4d_{12}$$
$$-6451200c_0c_2d_2d_{16} - 11289600c_0c_2d_4d_{14} - 14515200c_0c_2d_6d_{12} - 16128000c_0c_2d_8d_{10}$$
$$-5644800c_0c_4d_2d_{14} - 9676800c_0c_4d_4d_{12} - 12096000c_0c_4d_6d_{10} - 6451200c_0c_4d_8^2$$
$$-4838400c_0c_6d_2d_{12} - 8064000c_0c_6d_4d_{10} - 9676800c_0c_6d_6d_8 - 4032000c_0c_8d_2d_{10}$$
$$-6451200c_0c_8d_4d_8 - 3628800c_0c_8d_6^2 - 3225600c_0c_{10}d_2d_8 - 4838400c_0c_{10}d_4d_6$$
$$-2419200c_0c_{12}d_2d_6 - 1612800c_0c_{12}d_4^2 - 1612800d_2d_4c_0c_{14} - 403200d_2^2c_0c_{16}$$
$$-2822400c_2^2d_2d_{14} - 4838400c_2^2d_4d_{12} - 6048000c_2^2d_6d_{10} - 3225600c_2^2d_8^2 - 403200d_2^2c_6c_{10}$$
$$-4838400c_2c_4d_2d_{12} - 8064000c_2c_4d_4d_{10} - 9676800c_2c_4d_6d_8 - 4032000c_2c_6d_2d_{10}$$
$$-6451200c_2c_6d_4d_8 - 3628800c_2c_6d_6^2 - 3225600c_2c_8d_2d_8 - 4838400c_2c_8d_4d_6$$
$$-2419200c_2c_{10}d_2d_6 - 1612800c_2c_{10}d_4^2 - 1612800d_2d_4c_2c_{12} - 403200d_2^2c_2c_{14}$$
$$-2016000c_4^2d_2d_{10} - 3225600c_4^2d_4d_8 - 1814400c_4^2d_6^2 - 3225600c_4c_6d_2d_8$$
$$-4838400c_4c_6d_4d_6 - 2419200c_4c_8d_2d_6 - 1612800c_4c_8d_4^2 - 1612800d_2d_4c_4c_{10}$$
$$-403200d_2^2c_4c_{12} - 1209600c_6^2d_2d_6 - 806400c_6^2d_4^2 - 1612800d_2d_4c_6c_8 - 201600d_2^2c_8^2)$$

$$c_{20} = -\frac{1}{22176000c_0^2}(453600G^2H_0^2d_2d_{18} + 806400G^2H_0^2d_4d_{16} + 1058400G^2H_0^2d_6d_{14}$$
$$+1209600G^2H_0^2d_8d_{12} + 630000G^2H_0^2d_{10}^2 + 907200G^2H_0d_0d_2d_{18} + 1612800G^2H_0d_0d_4d_{16}$$
$$+2116800G^2H_0d_0d_6d_{14} + 2419200G^2H_0d_0d_8d_{12} + 408800G^2H_0d_2^2d_{16} + 966000G^2H_0d_2d_4d_{14}$$
$$+1260000G^2H_0d_0d_{10}^2 + 1101600G^2H_0d_2d_6d_{12} + 1176000G^2H_0d_2d_8d_{10} + 432000G^2H_0d_4^2d_{12}$$
$$+856800G^2H_0d_4d_6d_{10} + 430080G^2H_0d_4d_8^2 + 393120G^2H_0d_6^2d_8 + 453600G^2d_0^2d_2d_{18}$$
$$+806400G^2d_0^2d_4d_{16} + 1058400G^2d_0^2d_6d_{14} + 1209600G^2d_0^2d_8d_{12} + 630000G^2d_0^2d_{10}^2$$
$$+408800G^2d_0d_2^2d_{16} + 966000G^2d_0d_2d_4d_{14} + 1101600G^2d_0d_2d_6d_{12} + 1176000G^2d_0d_2d_8d_{10}$$
$$+432000G^2d_0d_4^2d_{12} + 856800G^2d_0d_4d_6d_{10} + 430080G^2d_0d_4d_8^2 + 393120G^2d_0d_6^2d_8$$
$$+91350G^2d_2^3d_{14} + 268800G^2d_2^2d_4d_{12} + 279300G^2d_2^2d_6d_{10} + 142128G^2d_2^2d_8^2$$
$$+224000G^2d_2d_4^2d_{10} + 426720G^2d_2d_4d_6d_8 + 66150G^2d_2d_6^3 + 58240G^2d_4^3d_8 + 81900G^2d_4^2d_6^2$$
$$+1260G^2H_0d_{18} + 1260G^2d_{18}d_0 + 700G^2d_{16}d_2 + 525G^2d_{14}d_4 + 450G^2d_{12}d_6 + 420G^2d_{10}d_8$$
$$-3628800c_0c_2d_2d_{18} - 6451200c_0c_2d_4d_{16} - 8467200c_0c_2d_6d_{14} - 9676800c_0c_2d_8d_{12}$$
$$-5040000c_0c_2d_{10}^2 - 3225600c_0c_4d_2d_{16} - 5644800c_0c_4d_4d_{14} - 7257600c_0c_4d_6d_{12}$$
$$-8064000c_0c_4d_8d_{10} - 2822400c_0c_6d_2d_{14} - 4838400c_0c_6d_4d_{12} - 6048000c_0c_6d_6d_{10}$$
$$-3225600c_0c_6d_8^2 - 2419200c_0c_8d_2d_{12} - 4032000c_0c_8d_4d_{10} - 4838400c_0c_8d_6d_8$$
$$-2016000c_0c_{10}d_2d_{10} - 3225600c_0c_{10}d_4d_8 - 1814400c_0c_{10}d_6^2 - 1612800c_0c_{12}d_2d_8$$
$$-2419200c_0c_{12}d_4d_6 - 1209600c_0c_{14}d_2d_6 - 806400c_0c_{14}d_4^2 - 806400c_0c_{16}d_2d_4$$
$$-201600c_0c_{18}d_2^2 - 1612800c_2^2d_2d_{16} - 2822400c_2^2d_4d_{14} - 3628800c_2^2d_6d_{12}$$
$$-4032000c_2^2d_8d_{10} - 2822400c_2c_4d_2d_{14} - 4838400c_2c_4d_4d_{12} - 6048000c_2c_4d_6d_{10}$$
$$-3225600c_2c_4d_8^2 - 2419200c_2c_6d_2d_{12} - 4032000c_2c_6d_4d_{10} - 4838400c_2c_6d_6d_8$$
$$-2016000c_2c_8d_2d_{10} - 3225600c_2c_8d_4d_8 - 1814400c_2c_8d_6^2 - 1612800c_2c_{10}d_2d_8$$
$$-2419200c_2c_{10}d_4d_6 - 1209600c_2c_{12}d_2d_6 - 806400c_2c_{12}d_4^2 - 806400c_2c_{14}d_2d_4$$
$$-201600c_2c_{16}d_2^2 - 1209600c_4^2d_2d_{12} - 2016000c_4^2d_4d_{10} - 2419200c_4^2d_6d_8$$
$$-2016000c_4c_6d_2d_{10} - 3225600c_4c_6d_4d_8 - 1814400c_4c_6d_6^2 - 1612800c_4c_8d_2d_8$$
$$-2419200c_4c_8d_4d_6 - 1209600c_4c_{10}d_2d_6 - 806400c_4c_{10}d_4^2 - 806400c_4c_{12}d_2d_4$$
$$-201600c_4c_{14}d_2^2 - 806400c_6^2d_2d_8 - 1209600c_6^2d_4d_6 - 1209600c_6c_8d_2d_6 - 806400c_6c_8d_4^2$$
$$-806400c_6c_{10}d_2d_4 - 201600c_6c_{12}d_2^2 - 403200c_8^2d_2d_4 - 201600c_8c_{10}d_2^2)$$

Appendix B

$$d_2 = -\frac{G(H_0 + d_0)}{4c_0},$$

$$d_4 = \frac{1}{64\,c_0^2}(4\,G^2H_0^2d_2 + 8\,G^2H_0d_0d_2 + 4\,G^2d_0^2d_2 + G^2H_0 + G^2d_0 - 32\,c_0c_2d_2),$$

$$d_6 = \frac{1}{1152\,c_0^2d_2}(192\,G^2H_0^2d_2d_4 + 384\,G^2H_0d_0d_2d_4 + 48\,G^2H_0d_2^3 + 192\,G^2d_0^2d_2d_4 + 48\,G^2d_0d_2^3$$
$$+8\,G^2H_0d_4 + 8\,G^2d_4d_0 + 3\,G^2d_2^2 - 768\,c_0^2d_4^2 - 1536\,c_0c_2d_2d_4 - 384\,c_0c_4d_2^2 - 192\,c_2^2d_2^2)$$

$$d_8 = \frac{1}{768\,c_0^2d_2}(144\,G^2H_0^2d_2d_6 + 96\,G^2H_0^2d_4^2 + 288\,G^2H_0d_0d_2d_6 + 192\,G^2H_0d_0d_4^2$$
$$+112\,G^2H_0d_2^2d_4 + 144\,G^2d_0^2d_2d_6 + 96\,G^2d_0^2d_4^2 + 112\,G^2d_0d_2^2d_4 + 6\,G^2d_2^4 + 3\,G^2H_0d_6$$
$$+3\,G^2d_6d_0 + 2\,G^2d_4d_2 - 1152\,c_0^2d_4d_6 - 1152\,c_0c_2d_2d_6 - 768\,c_0c_2d_4^2 - 768\,c_0c_4d_2d_4$$
$$-192\,c_0c_6d_2^2 - 384\,c_2^2d_2d_4 - 192\,c_2c_4d_2^2)$$

$$d_{10} = \frac{1}{28800c_0^2d_2}(5760G^2H_0^2d_2d_8 + 8640G^2H_0^2d_4d_6 + 11520G^2H_0d_0d_2d_8 + 17280G^2H_0d_0d_4d_6$$
$$+4680G^2H_0d_2^2d_6 + 4800G^2H_0d_2d_4^2 + 5760G^2d_0^2d_2d_8 + 8640G^2d_0^2d_4d_6 + 4680G^2d_0d_2^2d_6$$
$$+4800G^2d_0d_2d_4^2 + 960G^2d_2^3d_4 + 72G^2H_0d_8 + 72G^2d_0d_8 + 45G^2d_2d_6 + 20G^2d_4^2 - 46080c_0^2d_4d_8$$
$$-25920c_0^2d_6^2 - 46080c_0c_2d_2d_8 - 69120c_0c_2d_4d_6 - 34560c_0c_4d_2d_6 - 23040c_0c_2d_4^2 - 5760c_0c_8d_2^2$$
$$-23040c_0c_6d_2d_4 - 17280c_2^2d_2d_6 - 11520c_2^2d_4^2 - 23040c_2c_4d_2d_4 - 5760c_2c_6d_2^2 - 2880c_4^2d_2^2)$$

$$d_{12} = \frac{1}{17280 c_0^2 d_2} (3600 G^2 H_0^2 d_2 d_{10} + 5760 G^2 H_0^2 d_4 d_8 + 3240 G^2 H_0^2 d_6^2 + 7200 G^2 H_0 d_0 d_2 d_{10}$$
$$+ 11520 G^2 H_0 d_0 d_4 d_8 + 6480 G^2 H_0 d_0 d_6^2 + 3024 G^2 H_0 d_2^2 d_8 + 6480 G^2 H_0 d_2 d_4 d_6 + 960 G^2 H_0 d_4^3$$
$$+ 3600 G^2 d_0^2 d_2 d_{10} + 5760 G^2 d_0^2 d_4 d_8 + 3240 G^2 d_0^2 d_6^2 + 3024 G^2 d_0 d_2^2 d_8 + 6480 G^2 d_0 d_2 d_4 d_6$$
$$+ 960 G^2 d_0 d_4^3 + 630 G^2 d_2^3 d_6 + 880 G^2 d_2^2 d_4^2 + 30 G^2 H_0 d_{10} + 30 G^2 d_0 d_{10} + 18 G^2 d_2 d_8 + 15 G^2 d_4 d_6$$
$$- 28800 c_0^2 d_4 d_{10} - 34560 c_0^2 d_6 d_8 - 28800 c_0 c_2 d_2 d_{10} - 46080 c_0 c_2 d_4 d_8 - 25920 c_0 c_2 d_6^2$$
$$- 23040 c_0 c_4 d_2 d_8 - 34560 c_0 c_4 d_4 d_6 - 17280 c_0 c_6 d_2 d_6 - 11520 c_0 c_6 d_4^2 - 11520 c_0 c_8 d_2 d_4$$
$$- 2880 c_0 c_{10} d_2^2 - 11520 c_2^2 d_2 d_8 - 17280 c_2^2 d_4 d_6 - 17280 c_2 c_4 d_2 d_6 - 11520 c_2 c_4 d_4^2$$
$$- 11520 c_2 c_6 d_2 d_4 - 2880 c_2 c_8 d_2^2 - 5760 c_4^2 d_2 d_4 - 2880 c_4 c_6 d_2^2)$$

$$d_{14} = \frac{1}{1128960 c_0^2 d_2} (241920 G^2 H_0^2 d_2 d_{12} + 403200 G^2 H_0^2 d_4 d_{10} + 483840 G^2 H_0^2 d_6 d_8$$
$$+ 483840 G^2 H_0 d_0 d_2 d_{12} + 806400 G^2 H_0 d_0 d_4 d_{10} + 967680 G^2 H_0 d_0 d_6 d_8 + 208320 G^2 H_0 d_2^2 d_{10}$$
$$+ 462336 G^2 H_0 d_2 d_4 d_8 + 241920 G^2 H_0 d_2 d_6^2 + 201600 G^2 H_0 d_4^2 d_6 + 241920 G^2 d_0^2 d_2 d_{12}$$
$$+ 403200 G^2 d_0^2 d_4 d_{10} + 483840 G^2 d_0^2 d_6 d_8 + 208320 G^2 d_0 d_2^2 d_{10} + 462336 G^2 d_0 d_2 d_4 d_8$$
$$+ 241920 G^2 d_0 d_2 d_6^2 + 201600 G^2 d_0 d_4^2 d_6 + 44352 G^2 d_2^3 d_8 + 124320 G^2 d_2^2 d_4 d_6 + 35840 G^2 d_2 d_4^3$$
$$+ 1440 G^2 H_0 d_{12} + 1440 G^2 d_0 d_{12} + 840 G^2 d_2 d_{10} + 672 G^2 d_4 d_8 + 315 G^2 d_6^2 - 1935360 c_0^2 d_4 d_{12}$$
$$- 2419200 c_0^2 d_6 d_{10} - 1290240 c_0^2 d_8^2 - 1935360 c_0 c_2 d_2 d_{12} - 3225600 c_0 c_2 d_4 d_{10} - 3870720 c_0 c_2 d_6 d_8$$
$$- 1612800 c_0 c_4 d_2 d_{10} - 2580480 c_0 c_4 d_4 d_8 - 1451520 c_0 c_4 d_6^2 - 1290240 c_0 c_6 d_2 d_8$$
$$- 1935360 c_0 c_6 d_4 d_6 - 967680 c_0 c_8 d_2 d_6 - 645120 c_0 c_8 d_4^2 - 645120 c_0 c_{10} d_2 d_4 - 161280 c_0 c_{12} d_2^2$$
$$- 806400 c_2^2 d_2 d_{10} - 1290240 c_2^2 d_4 d_8 - 725760 c_2^2 d_6^2 - 1290240 c_2 c_4 d_2 d_8 - 1935360 c_2 c_4 d_4 d_6$$
$$- 967680 c_2 c_6 d_2 d_6 - 645120 c_2 c_6 d_4^2 - 645120 c_2 c_8 d_2 d_4 - 161280 c_2 c_{10} d_2^2 - 483840 c_4^2 d_2 d_6$$
$$- 322560 c_4^2 d_4^2 - 645120 c_4 c_6 d_2 d_4 - 161280 c_4 c_8 d_2^2 - 80640 c_6^2 d_2^2)$$

$$d_{16} = \frac{1}{322560 c_0^2 d_2} (70560 G^2 H_0^2 d_2 d_{14} + 120960 G^2 H_0^2 d_4 d_{12} + 151200 G^2 H_0^2 d_6 d_{10} + 315 G^2 H_0 d_{14}$$
$$+ 80640 G^2 H_0^2 d_8^2 + 141120 G^2 H_0 d_0 d_2 d_{14} + 241920 G^2 H_0 d_0 d_4 d_{12} + 302400 G^2 H_0 d_0 d_6 d_{10}$$
$$+ 161280 G^2 H_0 d_0 d_8^2 + 61920 G^2 H_0 d_2^2 d_{12} + 141120 G^2 H_0 d_2 d_4 d_{10} + 153216 G^2 H_0 d_2 d_6 d_8$$
$$+ 61824 G^2 H_0 d_4^2 d_8 + 60480 G^2 H_0 d_4 d_6^2 + 70560 G^2 d_0^2 d_2 d_{14} + 120960 G^2 d_0^2 d_4 d_{12} - 40320 c_6 c_8 d_2^2$$
$$+ 151200 G^2 d_0^2 d_6 d_{10} + 80640 G^2 d_0^2 d_8^2 + 61920 G^2 d_0 d_2^2 d_{12} + 141120 G^2 d_0 d_2 d_4 d_{10} + 2240 G^2 d_4^4$$
$$+ 153216 G^2 d_0 d_2 d_6 d_8 + 61824 G^2 d_0 d_4^2 d_8 + 60480 G^2 d_0 d_4 d_6^2 + 13440 G^2 d_2^3 d_{10} + 38304 G^2 d_2^2 d_4 d_8$$
$$+ 19215 G^2 d_2^2 d_6^2 + 31920 G^2 d_2 d_4^2 d_6 + 315 G^2 d_0 d_{14} + 180 G^2 d_2 d_{12} + 140 G^2 d_4 d_{10} + 126 G^2 d_6 d_8$$
$$- 564480 c_0 c_2 d_2 d_{14} - 967680 c_0 c_2 d_4 d_{12} - 1209600 c_0 c_2 d_6 d_{10} - 645120 c_0 c_2 d_8^2 - 483840 c_0 c_4 d_2 d_{12}$$
$$- 806400 c_0 c_4 d_4 d_{10} - 967680 c_0 c_4 d_6 d_8 - 403200 c_0 c_6 d_2 d_{10} - 645120 c_0 c_6 d_4 d_8 - 362880 c_0 c_6 d_6^2$$
$$- 322560 c_0 c_8 d_2 d_8 - 483840 c_0 c_8 d_4 d_6 - 241920 c_0 c_{10} d_2 d_6 - 161280 c_0 c_{10} d_4^2 - 161280 c_0 c_{12} d_2 d_4$$
$$- 40320 c_0 c_{14} d_2^2 - 241920 c_2^2 d_2 d_{12} - 40320 c_4 c_{10} d_2^2 - 403200 c_2^2 d_4 d_{10} - 483840 c_2^2 d_6 d_8$$
$$- 403200 c_2 c_4 d_2 d_{10} - 645120 c_2 c_4 d_4 d_8 - 362880 c_2 c_4 d_6^2 - 322560 c_2 c_6 d_2 d_8 - 483840 c_2 c_6 d_4 d_6$$
$$- 241920 c_2 c_8 d_2 d_6 - 161280 c_2 c_8 d_4^2 - 161280 c_2 c_{10} d_2 d_4 - 40320 c_2 c_{12} d_2^2 - 161280 c_4^2 d_2 d_8$$
$$- 80640 c_6^2 d_2 d_4 - 241920 c_4^2 d_4 d_6 - 241920 c_4 c_6 d_2 d_6 - 161280 c_4 c_6 d_4^2 - 161280 c_4 c_8 d_2 d_4)$$

$$d_{18} = \frac{1}{3628800 c_0^2 d_2}(806400 G^2 H_0^2 d_2 d_{16} + 1411200 G^2 H_0^2 d_4 d_{14} + 1814400 G^2 H_0^2 d_6 d_{12}$$
$$+2016000 G^2 H_0^2 d_8 d_{10} + 1612800 G^2 H_0 d_0 d_2 d_{16} + 2822400 G^2 H_0 d_0 d_4 d_{14}$$
$$+3628800 G^2 H_0 d_0 d_6 d_{12} + 4032000 G^2 H_0 d_0 d_8 d_{10} + 718200 d_2^2 G^2 d_{14} H_0$$
$$+1670400 G^2 H_0 d_2 d_4 d_{12} + 1864800 G^2 H_0 d_2 d_6 d_{10} + 967680 G^2 H_0 d_2 d_8^2$$
$$+739200 G^2 H_0 d_4^2 d_{10} + 1451520 G^2 H_0 d_4 d_6 d_8 + 226800 G^2 H_0 d_6^3 + 806400 G^2 d_0^2 d_2 d_{16}$$
$$+1411200 G^2 d_0^2 d_4 d_{14} + 1814400 G^2 d_0^2 d_6 d_{12} + 2016000 G^2 d_0^2 d_8 d_{10} + 718200 d_2^2 G^2 d_{14} d_0$$
$$+1670400 G^2 d_0 d_2 d_4 d_{12} + 1864800 G^2 d_0 d_2 d_6 d_{10} + 967680 G^2 d_0 d_2 d_8^2 + 739200 G^2 d_0 d_4^2 d_{10}$$
$$+1451520 G^2 d_0 d_4 d_6 d_8 + 226800 G^2 d_0 d_6^3 + 158400 G^2 d_2^3 d_{12} + 459200 G^2 d_2^2 d_4 d_{10}$$
$$+468720 G^2 d_2^2 d_6 d_8 + 380800 G^2 d_2 d_4^2 d_8 + 365400 G^2 d_2 d_4 d_6^2 + 100800 G^2 d_4^3 d_6$$
$$+2800 G^2 d_{16} H_0 + 2800 G^2 d_{16} d_0 + 1575 G^2 d_2 d_{14} + 1200 G^2 d_4 d_{12} + 1050 G^2 d_6 d_{10} + 504 G^2 d_8^2$$
$$-6451200 c_0 c_2 d_2 d_{16} - 11289600 c_0 c_2 d_4 d_{14} - 14515200 c_0 c_2 d_6 d_{12} - 16128000 c_0 c_2 d_8 d_{10}$$
$$-5644800 c_0 c_4 d_2 d_{14} - 9676800 c_0 c_4 d_4 d_{12} - 12096000 c_0 c_4 d_6 d_{10} - 6451200 c_0 c_4 d_8^2$$
$$-4838400 c_0 c_6 d_2 d_{12} - 8064000 c_0 c_6 d_4 d_{10} - 9676800 c_0 c_6 d_6 d_8 - 4032000 c_0 c_8 d_2 d_{10}$$
$$-6451200 c_0 c_8 d_4 d_8 - 3628800 c_0 c_8 d_6^2 - 3225600 c_0 c_{10} d_2 d_8 - 4838400 c_0 c_{10} d_4 d_6$$
$$-2419200 c_0 c_{12} d_2 d_6 - 1612800 c_0 c_{12} d_4^2 - 1612800 d_2 d_4 c_0 c_{14} - 403200 d_2^2 c_0 c_{16}$$
$$-2822400 c_2^2 d_2 d_{14} - 4838400 c_2^2 d_4 d_{12} - 6048000 c_2^2 d_6 d_{10} - 3225600 c_2^2 d_8^2$$
$$-4838400 c_2 c_4 d_2 d_{12} - 8064000 c_2 c_4 d_4 d_{10} - 9676800 c_2 c_4 d_6 d_8 - 4032000 c_2 c_6 d_2 d_{10}$$
$$-6451200 c_2 c_6 d_4 d_8 - 3628800 c_2 c_6 d_6^2 - 3225600 c_2 c_8 d_2 d_8 - 4838400 c_2 c_8 d_4 d_6$$
$$-2419200 c_2 c_{10} d_2 d_6 - 1612800 c_2 c_{10} d_4^2 - 1612800 d_2 d_4 c_2 c_{12} - 403200 d_2^2 c_2 c_{14}$$
$$-2016000 c_4^2 d_2 d_{10} - 3225600 c_4^2 d_4 d_8 - 1814400 c_4^2 d_6^2 - 3225600 c_4 c_6 d_2 d_8$$
$$-4838400 c_4 c_6 d_4 d_6 - 2419200 c_4 c_8 d_2 d_6 - 1612800 c_4 c_8 d_4^2 - 1612800 d_2 d_4 c_4 c_{10}$$
$$-403200 d_2^2 c_4 c_{12} - 1209600 c_6^2 d_2 d_6 - 806400 c_6^2 d_4^2 - 1612800 d_2 d_4 c_6 c_8$$
$$-403200 d_2^2 c_6 c_{10} - 201600 d_2^2 c_8^2)$$

$$d_{20} = \frac{1}{2016000 c_0^2 d_2}(453600 G^2 H_0^2 d_2 d_{18} + 806400 G^2 H_0^2 d_4 d_{16} + 1058400 G^2 H_0^2 d_6 d_{14}$$
$$+1209600 G^2 H_0^2 d_8 d_{12} + 630000 G^2 H_0^2 d_{10}^2 + 907200 G^2 H_0 d_0 d_2 d_{18} + 1612800 G^2 H_0 d_0 d_4 d_{16}$$
$$+2116800 G^2 H_0 d_0 d_6 d_{14} + 2419200 G^2 H_0 d_0 d_8 d_{12} + 1260000 G^2 H_0 d_0 d_{10}^2 + 408800 G^2 H_0 d_2^2 d_{16}$$
$$+966000 G^2 H_0 d_2 d_4 d_{14} + 1101600 G^2 H_0 d_2 d_6 d_{12} + 1176000 G^2 H_0 d_2 d_8 d_{10} + 432000 G^2 H_0 d_4^2 d_{12}$$
$$+856800 G^2 H_0 d_4 d_6 d_{10} + 430080 G^2 H_0 d_4 d_8^2 + 393120 G^2 H_0 d_6^2 d_8 + 453600 G^2 d_0^2 d_2 d_{18}$$
$$+806400 G^2 d_0^2 d_4 d_{16} + 1058400 G^2 d_0^2 d_6 d_{14} + 1209600 G^2 d_0^2 d_8 d_{12} + 630000 G^2 d_0^2 d_{10}^2$$
$$+408800 G^2 d_0 d_2^2 d_{16} + 966000 G^2 d_0 d_2 d_4 d_{14} + 1101600 G^2 d_0 d_2 d_6 d_{12} + 1176000 G^2 d_0 d_2 d_8 d_{10}$$
$$+432000 G^2 d_0 d_4^2 d_{12} + 856800 G^2 d_0 d_4 d_6 d_{10} + 430080 G^2 d_0 d_4 d_8^2 + 393120 G^2 d_0 d_6^2 d_8$$
$$+91350 G^2 d_2^3 d_{14} + 268800 G^2 d_2^2 d_4 d_{12} + 279300 G^2 d_2^2 d_6 d_{10} + 142128 G^2 d_2^2 d_8^2$$
$$+224000 G^2 d_2 d_4^2 d_{10} + 426720 G^2 d_2 d_4 d_6 d_8 + 66150 G^2 d_2 d_6^3 + 58240 G^2 d_4^3 d_8 + 81900 G^2 d_4^2 d_6^2$$
$$+1260 G^2 H_0 d_{18} + 1260 G^2 d_{18} d_0 + 700 G^2 d_{16} d_2 + 525 G^2 d_{14} d_4 + 450 G^2 d_{12} d_6 + 420 G^2 d_{10} d_8$$
$$-3628800 c_0 c_2 d_2 d_{18} - 6451200 c_0 c_2 d_4 d_{16} - 8467200 c_0 c_2 d_6 d_{14} - 9676800 c_0 c_2 d_8 d_{12}$$
$$-5040000 c_0 c_2 d_{10}^2 - 3225600 c_0 c_4 d_2 d_{16} - 5644800 c_0 c_4 d_4 d_{14} - 7257600 c_0 c_4 d_6 d_{12}$$
$$-8064000 c_0 c_4 d_8 d_{10} - 2822400 c_0 c_6 d_2 d_{14} - 4838400 c_0 c_6 d_4 d_{12} - 6048000 c_0 c_6 d_6 d_{10}$$
$$-3225600 c_0 c_6 d_8^2 - 2419200 c_0 c_8 d_2 d_{12} - 4032000 c_0 c_8 d_4 d_{10} - 4838400 c_0 c_8 d_6 d_8$$
$$-2016000 c_0 c_{10} d_2 d_{10} - 3225600 c_0 c_{10} d_4 d_8 - 1814400 c_0 c_{10} d_6^2 - 1612800 c_0 c_{12} d_2 d_8$$
$$-2419200 c_0 c_{12} d_4 d_6 - 1209600 c_0 c_{14} d_2 d_6 - 806400 c_0 c_{14} d_4^2 - 806400 c_0 c_{16} d_2 d_4$$
$$-201600 c_0 c_{18} d_2^2 - 1612800 c_2^2 d_2 d_{16} - 2822400 c_2^2 d_4 d_{14} - 3628800 c_2^2 d_6 d_{12}$$
$$-4032000 c_2^2 d_8 d_{10} - 2822400 c_2 c_4 d_2 d_{14} - 4838400 c_2 c_4 d_4 d_{12} - 6048000 c_2 c_4 d_6 d_{10}$$
$$-3225600 c_2 c_4 d_8^2 - 2419200 c_2 c_6 d_2 d_{12} - 4032000 c_2 c_6 d_4 d_{10} - 4838400 c_2 c_6 d_6 d_8$$
$$-2016000 c_2 c_8 d_2 d_{10} - 3225600 c_2 c_8 d_4 d_8 - 1814400 c_2 c_8 d_6^2 - 1612800 c_2 c_{10} d_2 d_8$$
$$-2419200 c_2 c_{10} d_4 d_6 - 1209600 c_2 c_{12} d_2 d_6 - 806400 c_2 c_{12} d_4^2 - 806400 c_2 c_{14} d_2 d_4$$
$$-201600 c_2 c_{16} d_2^2 - 1209600 c_4^2 d_2 d_{12} - 2016000 c_4^2 d_4 d_{10} - 2419200 c_4^2 d_6 d_8$$
$$-2016000 c_4 c_6 d_2 d_{10} - 3225600 c_4 c_6 d_4 d_8 - 1814400 c_4 c_6 d_6^2 - 1612800 c_4 c_8 d_2 d_8$$
$$-2419200 c_4 c_8 d_4 d_6 - 1209600 c_4 c_{10} d_2 d_6 - 806400 c_4 c_{10} d_4^2 - 806400 c_4 c_{12} d_2 d_4$$
$$-201600 c_4 c_{14} d_2^2 - 806400 c_6^2 d_2 d_8 - 1209600 c_6^2 d_4 d_6 - 1209600 c_6 c_8 d_2 d_6 - 806400 c_6 c_8 d_4^2$$
$$-806400 c_6 c_{10} d_2 d_4 - 201600 c_6 c_{12} d_2^2 - 403200 c_8^2 d_2 d_4 - 201600 c_8 c_{10} d_2^2)$$

Appendix C

$$b_1 = \frac{1}{D - ad_0},$$

$$b_3 = \frac{b_1 d_2}{a(D - ad_0)},$$

$$b_5 = \frac{1}{a^3(D - ad_0)}(a^2 b_3 d_2 + b_1 d_4),$$

$$b_7 = \frac{1}{a^5(D - ad_0)}(a^4 b_5 d_2 + a^2 b_3 d_4 + b_1 d_6),$$

$$b_9 = \frac{1}{a^7(D - ad_0)}(a^6 b_7 d_2 + a^4 b_5 d_4 + a^2 b_3 d_6 + b_1 d_8),$$

$$b_{11} = \frac{1}{a^9(D - ad_0)}(a^8 b_9 d_2 + a^6 b_7 d_4 + a^4 b_5 d_6 + a^2 b_3 d_8 + b_1 d_{10}),$$

$$b_{13} = \frac{1}{a^{11}(D - ad_0)}(a^{10} b_{11} d_2 + a^8 b_9 d_4 + a^6 b_7 d_6 + a^4 b_5 d_8 + a^2 b_3 d_{10} + b_1 d_{12}),$$

$$b_{15} = \frac{1}{a^{13}(D - ad_0)}(a^{12} b_{13} d_2 + a^{10} b_{11} d_4 + a^8 b_9 d_6 + a^6 b_7 d_8 + a^4 b_5 d_{10} + a^2 b_3 d_{12} + b_1 d_{14}),$$

$$b_{17} = \frac{1}{a^{15}(D - ad_0)}(b_{15} d_2 a^{14} + b_{13} d_4 a^{12} + b_{11} d_6 a^{10} + b_9 d_8 a^8 + b_7 d_{10} a^6 + b_5 d_{12} a^4 + b_3 d_{14} a^2 + b_1 d_{16}),$$

$$b_{19} = \frac{1}{a^{17}(D - ad_0)}(b_{17} d_2 a^{16} + b_{15} d_4 a^{14} + b_{13} d_6 a^{12} + b_{11} d_8 a^{10} + b_9 d_{10} a^8 + b_7 d_{12} a^6 + b_5 d_{14} a^4 + b_3 d_{16} a^2 + b_1 d_{18})$$

$$b_{21} = \frac{1}{a^{19}(D - ad_0)}(b_{19} d_2 a^{18} + b_{17} d_4 a^{16} + b_{15} d_6 a^{14} + b_{13} d_8 a^{12} + b_{11} d_{10} a^{10} + b_9 d_{12} a^8 + b_7 d_{14} a^6 + b_5 d_{16} a^4 + b_3 d_{18} a^2 + b_1 d_{20})$$

References

1. Bernardo, P.; Iulianelli, A.; Macedonio, F.; Drioli, E. Membrane technologies for space engineering. *J. Membrane Sci.* **2021**, *626*, 119177. [CrossRef]
2. Suresh, K.; Katara, N. Design and development of circular ceramic membrane for wastewater treatment. *Mater. Today Proc.* **2021**, *43*, 2176–2181. [CrossRef]
3. Tai, Y.; Zhou, K.; Chen, N. Dynamic Properties of Microresonators with the Bionic Structure of Tympanic Membrane. *Sensors* **2020**, *20*, 6958. [CrossRef]
4. Dadgar-Rad, F.; Imani, A. Theory of gradient-elastic membranes and its application in the wrinkling analysis of stretched thin sheets. *J. Mech. Phys. Solids* **2019**, *132*, 103679. [CrossRef]
5. Li, X.; Sun, J.-Y.; Lu, X.-C.; Yang, Z.-X.; He, X.-T. Steady fluid–structure coupling interface of circular membrane under liquid weight loading: Closed-form solution for differential-integral equations. *Mathematics* **2021**, *9*, 1105. [CrossRef]
6. Dai, Z.; Lu, N. Poking and bulging of suspended thin sheets: Slippage, instabilities, and metrology. *J. Mech. Phys. Solids* **2021**, *149*, 104320. [CrossRef]
7. Liu, T.; Wang, X.H.; Qiu, X.M.; Zhang, X.H. Theoretical study on the parameter sensitivity over the mechanical states of inflatable membrane antenna. *Aerosp. Sci. Technol.* **2020**, *102*, 105843. [CrossRef]
8. Williams, J.G. Energy release rates for the peeling of flexible membranes and the analysis of blister tests. *Int. J. Fract.* **1997**, *87*, 265–288. [CrossRef]
9. Wang, J.; Lou, Y.; Wang, B.; Sun, Q.; Zhou, M.; Li, X. Highly sensitive, breathable, and flexible pressure sensor based on electrospun membrane with assistance of AgNW/TPU as composite dielectric layer. *Sensors* **2020**, *20*, 2459. [CrossRef]
10. Lian, Y.-S.; Sun, J.-Y.; Zhao, Z.-H.; Li, S.-Z.; Zheng, Z.-L. A refined theory for characterizing adhesion of elastic coatings on rigid substrates based on pressurized blister test methods: Closed-form solution and energy release rate. *Polymers* **2020**, *12*, 1788. [CrossRef]

11. Li, X.; Sun, J.-Y.; Shi, B.-B.; Zhao, Z.-H.; He, X.-T. A theoretical study on an elastic polymer thin film-based capacitive wind-pressure sensor. *Polymers* **2020**, *12*, 2133. [CrossRef] [PubMed]

12. Jindal, S.K.; Varma, M.A.; Thukral, D. Comprehensive assessment of MEMS double touch mode capacitive pressure sensor on utilization of SiC film as primary sensing element: Mathematical modelling and numerical simulation. *Microelectron. J.* **2018**, *73*, 30–36. [CrossRef]

13. Lee, H.Y.; Choi, B. Theoretical and experimental investigation of the trapped air effect on air-sealed capacitive pressure sensor. *Sens. Actuat. A-Phys.* **2015**, *221*, 104–114. [CrossRef]

14. Liao, M.; Liao, A.; Liu, J.; Cai, Z.; Liu, H.; Ma, T. A novel method and system for the fast calibration of tipping bucket rain gauges. *J. Hydrol.* **2021**, *597*, 125782. [CrossRef]

15. Sypka, P. Dynamic real-time volumetric correction for tipping-bucket rain gauges. *Agric. For. Meteorol.* **2019**, *271*, 158–167. [CrossRef]

16. Yang, Z.-X.; Sun, J.-Y.; Zhao, Z.-H.; Li, S.-Z.; He, X.-T. A closed-form solution of prestressed annular membrane internally-connected with rigid circular plate and transversely-loaded by central shaft. *Mathematics* **2020**, *8*, 521. [CrossRef]

17. Khapin, A.V.; Abdeev, B.M.; Makhiyev, B.E. Optimal size of an axisymmetric perfectly flexible membrane with a rigid centre loaded with a concentrated static force. *IOP Conf. Ser. Mater. Sci. Eng.* **2020**, *775*, 012138. [CrossRef]

18. Yang, Z.-X.; He, X.-T.; Wen, S.-R. Closed-form solution and experimental verification for the axisymmetric deformation problem of blistering circular thin polymer films under uniformly distributed gas pressure. *Polymers* **2020**, *12*, 1130. [CrossRef]

19. Huang, P.F.; Song, Y.P.; Li, Q.; Liu, X.Q.; Feng, Y.Q. A theoretical study of circular orthotropic membrane under concentrated load: The relation of load and deflection. *IEEE Access* **2020**, *8*, 126127–126137. [CrossRef]

20. Lian, Y.S.; Sun, J.Y.; Dong, J.; Zheng, Z.L.; Yang, Z.X. Closed-form solution of axisymmetric deformation of prestressed Föppl-Hencky membrane under constrained deflecting. *Struct. Eng. Mech.* **2019**, *69*, 693–698.

21. Chen, S.L.; Zheng, Z.L. Large deformation of circular membrane under the concentrated force. *Appl. Math. Mech.* **2003**, *24*, 28–31.

22. Hencky, H. On the stress state in circular plates with vanishing bending stiffness. *Z. Angew. Math. Phys.* **1915**, *63*, 311–317. (In German)

23. Chien, W.Z.; Wang, Z.Z.; Xu, Y.G.; Chen, S.L. The symmetrical deformation of circular membrane under the action of uniformly distributed loads in its portion. *Appl. Math. Mech.* **1981**, *2*, 653–668.

24. Sun, J.Y.; Rong, Y.; He, X.T.; Gao, X.W.; Zheng, Z.L. Power series solution of circular membrane under uniformly distributed loads: Investigation into Hencky transformation. *Stuct. Eng. Mech.* **2013**, *45*, 631–641. [CrossRef]

25. Sun, J.Y.; Lian, Y.S.; Li, Y.M.; He, X.T.; Zheng, Z.L. Closed-form solution of elastic circular membrane with initial stress under uniformly-distributed loads: Extended Hencky solution. *Z. Angew. Math. Mech.* **2015**, *95*, 1335–1341. [CrossRef]

26. Ma, Y.; Wang, G.R.; Chen, Y.L.; Long, D.; Guan, Y.C.; Liu, L.Q.; Zhang, Z. Extended Hencky solution for the blister test of nanomembrane. *Extreme Mech. Lett.* **2018**, *22*, 69–78. [CrossRef]

27. Li, X.; Sun, J.-Y.; Zhao, Z.-H.; He, X.-T. Large deflection analysis of axially symmetric deformation of prestressed circular membranes under uniform lateral loads. *Symmetry* **2020**, *12*, 1343. [CrossRef]

28. Mei, D.; Sun, J.-Y.; Zhao, Z.-H.; He, X.-T. A closed-form solution for the boundary value problem of gas pressurized circular membranes in contact with frictionless rigid plates. *Mathematics* **2020**, *8*, 1017. [CrossRef]

29. Shi, B.-B.; Sun, J.-Y.; Huang, T.-K.; He, X.-T. Closed-form solution for circular membranes under in-plane radial stretching or compressing and out-of-plane gas pressure loading. *Mathematics* **2021**, *9*, 1238. [CrossRef]

30. Antonova, I.; Nebogatikova, N.; Zerrouki, N.; Kurkina, I.; Ivanov, A. Flexibility of Fluorinated Graphene-Based Materials. *Materials* **2020**, *13*, 1032. [CrossRef]

31. Chulkin, P.; Łapkowski, M. An Insight into Ionic Conductivity of Polyaniline Thin Films. *Materials* **2020**, *13*, 2877. [CrossRef] [PubMed]

32. Molla-Alipour, M.; Ganji, B.A. Analytical analysis of mems capacitive pressure sensor with circular diaphragm under dynamic load using differential transformation method (DTM). *Acta Mech. Solida Sin.* **2015**, *28*, 400–408. [CrossRef]